Unpolarized quark and gluon TMD PDFs and FFs at N3LO

Luo, Ming-xing ; Yang, Tong-Zhi ; Zhu, Hua Xing ; Zhu, Yu Jiao

Abstract: In this paper we calculate analytically the perturbative matching coefficients for unpolarized quark and gluon Transverse-Momentum-Dependent (TMD) Parton Distribution Functions (PDFs) and Fragmentation Functions (FFs) through Next-to-Next-to-Next-to-Leading Order (N3LO) in QCD. The N3LO TMD PDFs are calculated by solving a system of differential equation of Feynman and phase space integrals. The TMD FFs are obtained by analytic continuation from space-like quantities to time-like quantities, taking into account the probability interpretation of TMD PDFs and FFs properly. The coefficient functions for TMD FFs exhibit double logarithmic enhancement at small momentum fraction z. We resum such logarithmic terms to the third order in the expansion of s. Our results constitute important ingredients for precision determination of TMD PDFs and FFs in current and future experiments.

DOI: https://doi.org/10.1007/jhep06(2021)115

Originally published at:
Luo, Ming-xing; Yang, Tong-Zhi; Zhu, Hua Xing; Zhu, Yu Jiao (2021). Unpolarized quark and gluon TMD PDFs and FFs at N3LO. Journal of High Energy Physics, 2021(6):115.
DOI: https://doi.org/10.1007/jhep06(2021)115

Published for SISSA by Springer

Received: March 15, 2021
Accepted: May 11, 2021
Published: June 17, 2021

Unpolarized quark and gluon TMD PDFs and FFs at N^{3}LO

Ming-xing Luo,[a,b] **Tong-Zhi Yang,**[c,a] **Hua Xing Zhu**[a] **and Yu Jiao Zhu**[a]

[a] *Zhejiang Institute of Modern Physics, Department of Physics, Zhejiang University, Hangzhou, 310027, China*

[b] *Complex Systems Division, Beijing Computational Science Research Center, Beijing, 100193, China*

[c] *Department of Physics, University of Zürich, CH-8057 Zürich, Switzerland*

E-mail: mingxingluo@zju.edu.cn, yangtz@zju.edu.cn, zhuhx@zju.edu.cn, zhuyujiao@zju.edu.cn

Abstract: In this paper we calculate analytically the perturbative matching coefficients for unpolarized quark and gluon Transverse-Momentum-Dependent (TMD) Parton Distribution Functions (PDFs) and Fragmentation Functions (FFs) through Next-to-Next-to-Next-to-Leading Order (N^{3}LO) in QCD. The N^{3}LO TMD PDFs are calculated by solving a system of differential equation of Feynman and phase space integrals. The TMD FFs are obtained by analytic continuation from space-like quantities to time-like quantities, taking into account the probability interpretation of TMD PDFs and FFs properly. The coefficient functions for TMD FFs exhibit double logarithmic enhancement at small momentum fraction z. We resum such logarithmic terms to the third order in the expansion of α_s. Our results constitute important ingredients for precision determination of TMD PDFs and FFs in current and future experiments.

Keywords: Perturbative QCD, Resummation

ArXiv ePrint: 2012.03256

https://doi.org/10.1007/JHEP06(2021)115

JHEP06(2021)115

Contents

1 Introduction

Understanding the parton structures of hadron is one of the outstanding problem in Quantum ChromodyDynamics (QCD). TMD PDFs and FFs describe the distribution of parton transverse momentum inside a hadron in parton scattering or decay. Their knowledge is essential to our understanding of the confined motion of parton in nucleons [1–3]. Thanks to factorization and evolution [4–15], TMD PDFs and FFs also enter high precision theoretical prediction for a large variety of observables at high energy colliders. From pure theoretical point of view, TMD PDFs and FFs are also interesting since they represent light-cone correlation of quantum fields with intrinsic space-like and time-like origin, respectively. Their transparent definition in terms of light-cone correlator also allow higher-order perturbative calculation, from which one can uncover interesting analytic structure of the correlators.

In the past decade perturbative calculations for TMD distributions have seen rapid development. Next-to-Next-to-Leading Order (NNLO) corrections to TMD PDFs are first obtained by extraction from expansion of Drell-Yan and Higgs p_T distribution in the relevant

JHEP06(2021)115

kinemtical limit [16, 17]. Direct calculation of TMD PDFs and FFs from their light-cone operator definition is difficult due to the existence of unregulated rapidity singularities. Much efforts have been devoted to the inclusion of rapidity regulator and its associated rapidity factorization [7, 9, 12, 13, 15, 18–22]. Using rapidity regulators, direct computation of TMD PDFs and FFs at NNLO have since become available [23–28]. The progress in NNLO calculation for TMD distributions have allowed many cutting-edge calculations for phenomenology, including fixed-order calculation at NNLO and beyond [29–34] and resummation for large logarithms at small q_T at unprecedented $\mathrm{N^3LL}$ accuracy [34–41]. We also note that perturbative calculation for TMD quantities suitable for lattice calculation [42–45] has also made important progress recently [46].

Recently a first step towards $\mathrm{N^3LO}$ TMD distributions have been achieved in [47] by calculating the unpolarized quark TMD PDFs, extending and significantly improving upon the methods in [26, 27]. Subsequently, both unpolarized quark and gluon TMD PDFs are obtained in [48], based on an independent method from [49]. In this paper we continue our calculation in [47], and present the $\mathrm{N^3LO}$ results for unpolarized quark TMD FFs, and unpolarized gluon TMD PDFs and FFs. We also present the results for unpolarized quark TMD PDFs from [47] for completeness.

Our method for calculating the unpolarized gluon TMD PDFs follows [47]. In order to obtain the results for TMD FFs, we adopt a strategy of analytic continuation proposed in [50]. The crucial observation is that although TMD PDFs or FFs are not themselves analytic function of momentum fraction, but the building blocks, space-like and time-like splitting amplitudes, are. At $\mathrm{N^3LO}$, there are four distinct contributions to TMD PDFs or FFs, namely the triple real part, the double real-virtual part, the double virtual-real part, and the virtual squared-real part. Ref. [50] shows that (a) the analytic continuation for the triple real part is trivial since it doesn't involve loop integrals; (b) the analytic continuation for the double real-virtual is also trivial at this order since the continuation of virtual loop only generate $i\pi$ terms which cancel in the sum with complex conjugate. (c) the analytic continuation of double virtual-real part and virtual squared-real part is non-trivial. But they are also simple to calculate since they only involve a one-particle phase space integral. It is suggested in [50] that one can calculate these two parts using the corresponding space-like or time-like splitting amplitudes, instead of trying to analytically continue them. Using this approach, ref. [50] determines the complete time-like splitting functions at NNLO from the space-like counterpart, including the off-diagonal $P_{qg}^{T(2)}$, which cannot be completely fixed with previous methods [51–53]. With the complete NNLO time-like splitting functions, ref. [50] also provides striking evidence for the existence of a generalized Gribov-Lipatov reciprocity relation between space-like and time-like QCD splitting functions in both non-singlet and singlet sector through NNLO. In this paper we use the idea of ref. [50] to determine not just the splitting functions, but the full time-like TMD FFs through $\mathrm{N^3LO}$. Our results for TMD PDFs and FFs are written in terms of familiar harmonic polylogarithms [54] up to transcendental weight 5 and allow convenient analytical and numerical manipulation. We provide analytic expression for TMD PDFs and FFs in the threshold limit ($x\,, z \to 1$) and high energy limit ($x\,, z \to 0$). In the high energy limit, TMD FFs exhibit double logarithmic enhancement, instead of single logarithmic

JHEP06(2021)115

enhancement as the in the case of TMD PDFs. A recent discussion of the enhanced double logarithms can be found in [55]. We resum the large $\ln z$ terms in TMD FFs to the third order in the expansion of strong coupling, following the method of Vogt [56, 57]. We note that a different method based on celestial BFKL equation has also been developed to resum the time-like small-z logarithms to NNLL in [55].

The structure of this paper is as follows. In section 2 we give the necessary operator definition and renormalization for TMD PDFs and FFs. In section 3 we present the N^{3}LO results for unpolarized quark and gluon TMD PDFs and FFs. Since the expressions are lengthy, we present in the text only a numerical fit to these functions, valid to 0.1 percent in the range of $0 < x\,, z < 1$. The full analytic expressions are provided as supplementary material attached to this paper. We also give the analytic expressions in the threshold limit in this section. In section 4 we investigate the high energy limit of TMD PDFs and FFs, $x\,, z \to 0$. We provide explicit analytic expressions, showing that TMD FFs are more singular than TMD PDFs from fixed-order point of view, namely double logs in contrast to single logs. We resum the small z logarithms for TMD FFs to the third order in the expansion of α_s. We conclude in section 5.

2 Definition of quark and gluon TMD PDFs and FFs

In this section we give the necessary operator defintion for unpolarized quark and gluon TMD PDFs and FFs. We also give the renormalization counter terms and specify the zero-bin subtraction.

2.1 Operator definitions for TMD PDFs

We begin with the bare TMD PDFs for unpolarized quark and gluon, which can be defined in terms of SCET [58–62] collinear fields

$$\begin{aligned}\mathcal{B}^{\rm bare}_{q/N}(x,b_\perp) &= \int \frac{db^-}{2\pi}\, e^{-ixb^-P^+} \langle N(P)|\bar{\chi}_n(0,b^-,b_\perp)\frac{\bar{\not{n}}}{2}\chi_n(0)|N(P)\rangle\,,\\ \mathcal{B}^{\rm bare,\mu\nu}_{g/N}(x,b_\perp) &= -\,xP_+\int \frac{db^-}{2\pi} e^{-ixb^-P^+} \langle N(P)|\mathcal{A}^{a,\mu}_{n\perp}(0,b^-,b_\perp)\mathcal{A}^{a,\nu}_{n\perp}(0)|N(P)\rangle\,,\end{aligned} \tag{2.1}$$

where $N(P)$ is a hadron state with momentum $P^\mu = (\bar{n}\cdot P)n^\mu/2 = P^+n^\mu/2$, with $n^\mu = (1,0,0,1)$ and $\bar{n}^\mu = (1,0,0,-1)$, $\chi_n = W_n^\dagger \xi_n$ is the gauge invariant collinear quark field [63] in SCET, constructed from collinear quark field ξ_n and path-ordered collinear Wilson line $W_n(x) = \mathcal{P}\exp\left(ig\int_{-\infty}^0 ds\,\bar{n}\cdot A_n(x+\bar{n}s)\right)$, and $\mathcal{A}^{a,\mu}_{n\perp}$ is the gauge invariant collinear gluon field with color index a and Lorentz index μ.

For sufficiently small $b_\perp$, the TMD PDFs in eq. (2.1) admit operator product expansion onto the usual collinear PDFs,

$$\begin{aligned}\mathcal{B}^{\rm bare}_{q/N}(x,b_\perp) &= \sum_i \int_x^1 \frac{d\xi}{\xi}\,\mathcal{I}^{\rm bare}_{qi}(\xi,b_\perp)\,\phi^{\rm bare}_{i/N}(x/\xi) + \text{power corrections}\,,\\ \mathcal{B}^{\rm bare,\mu\nu}_{g/N}(x,b_\perp) &= \sum_i \int_x^1 \frac{d\xi}{\xi}\mathcal{I}^{\rm bare,\mu\nu}_{gi}(\xi,b_\perp)\phi^{\rm bare}_{i/N}(x/\xi) + \text{power corrections}\,,\end{aligned} \tag{2.2}$$

where the summation is over all parton flavors i. The perturbative matching coefficients $\mathcal{I}_{qi}^{\text{bare}}(\xi, b_\perp)$ and $\mathcal{I}_{gi}^{\text{bare},\mu\nu}(\xi, b_\perp)$ in eq. (2.2) are independent of the actual hadron N. In practical calculations, one can replace the hadron N with a partonic state j. Furthermore, the usual bare partonic collinear PDFs are just $\phi_{i/j}^{\text{bare}}(x) = \delta_{ij}\delta(1-x)$, therefore

$$\mathcal{I}_{qi}^{\text{bare}}(x, b_\perp) = \mathcal{B}_{qi}^{\text{bare}}(x, b_\perp)\,, \qquad \mathcal{I}_{gi}^{\text{bare},\mu\nu}(x, b_\perp) = \mathcal{B}_{gi}^{\text{bare},\mu\nu}(x, b_\perp) \tag{2.3}$$

up to power correction terms.

For gluon coefficient functions, one can perform a further decomposition into two independent Lorentz structures in $d = 4-2\epsilon$ dimension,

$$\mathcal{I}_{gi}^{\text{bare},\mu\nu}(\xi, b_\perp) = \frac{g_\perp^{\mu\nu}}{d-2}\mathcal{I}_{gi}^{\text{bare}}(\xi, b_T) + \left(\frac{g_\perp^{\mu\nu}}{d-2} + \frac{b_\perp^\mu b_\perp^\nu}{b_T^2}\right)\mathcal{I}'^{\text{bare}}_{gi}(\xi, b_T)\,, \tag{2.4}$$

where we have defined two scalar form factors, $\mathcal{I}_{gi}^{\text{bare}}$, the unpolarized gluon coefficient functions, and $\mathcal{I}'^{\text{bare}}_{gi}$, the linearly-polarized gluon coefficient functions. They can be projected out using

$$\begin{aligned}\mathcal{I}_{gi}^{\text{bare}}(\xi, b_T) &= g_\perp^{\mu\nu}\mathcal{I}_{gi}^{\text{bare},\mu\nu}(\xi, b_\perp)\,,\\ \mathcal{I}'^{\text{bare}}_{gi}(\xi, b_T) &= \frac{1}{d-3}\left[g_\perp^{\mu\nu} + (d-2)\,\frac{b_\perp^\mu b_\perp^\nu}{b_T^2}\right]\mathcal{I}_{gi}^{\text{bare},\mu\nu}(\xi, b_\perp)\,,\end{aligned} \tag{2.5}$$

with $b_T^2 = -b_\perp^2 > 0$ and $b_T = \sqrt{b_T^2}$. We focus on unpolarized TMD distributions for the current paper, and the results for the linearly-polarized gluon distribution are left for future work.

2.2 Operator definitions for TMD FFs

To specify the definition for gluon TMD FFs, it is necessary to specify a reference frame first. This is in contrast to PDFs, where the incoming hadron provides a canonical reference frame for transverse momentum. In the case of TMD FFs, two different frames can be defined, the hadron frame and the parton frame [12, 26, 27]. In the hadron frame, where the detected hadron has zero transverse momentum, an operator definition for gluon TMD FFs can be written down

$$\begin{aligned}\mathcal{D}_{N/q}^{\text{bare}}(z, b_\perp) &= \frac{1}{z}\sum_X\int\frac{db^-}{2\pi}e^{iP^+b^-/z}\langle 0|\bar\chi_n(0,b^-,b_\perp)|N(P),X\rangle\frac{\not{\bar n}}{2}\langle N(P),X|\chi_n(0)|0\rangle\,,\\ \mathcal{D}_{N/g}^{\text{bare},\mu\nu}(z, b_\perp) &= -\frac{P_+}{z^2}\sum_X\int\frac{db^-}{2\pi}e^{iP^+b^-/z}\langle 0|\mathcal{A}_{n\perp}^{a,\mu}(0,b^-,b_\perp)|N(P),X\rangle\langle N(P),X|\mathcal{A}_{n\perp}^{a,\nu}(0)|0\rangle\,,\end{aligned} \tag{2.6}$$

where $P^\mu = (\bar n\cdot P)n^\mu/2 = P^+n^\mu/2$ is the momenta of the final state detected hadron. Again, we focus on unpolarized partonic TMD distributions, the projection to unpolarized gluon distributions as in eq. (2.4) is understood from now on.

In practical calculations, in particular for FF renormalization, it's also convenient to define the fragmentation functions in the parton frame, where the parton which initiates

JHEP06(2021)115

the fragmentation has zero transverse momentum. The parton frame TMDFFs are related to the hadron frame ones by [12, 26]

$$\mathcal{F}^{\text{bare}}_{j/i}(z, b_\perp/z) = z^{2-2\epsilon}\mathcal{D}^{\text{bare}}_{j/i}(z, b_\perp)\,, \tag{2.7}$$

where we denote the bare partonic TMD FFs in the parton frame by $\mathcal{F}^{\text{bare}}_{j/i}$. Our N^{3}LO results for TMD FFs will be given in the hadron frame, by choosing the argument of the parton frame coefficient to be $b_\perp/z$.

2.3 Renormalization counter terms and zero-bin subtraction

The TMD PDFs or TMD FFs, as well as their matching coefficients, contain both UV and rapidity divergences. We adopt dimensional regularization for the UV, and exponentional regularization [21] for the rapidity divergences. After coupling constant renormalization in $\overline{\text{MS}}$ scheme, the α_s-renormalized matching coefficients still contains overlapping contributions between collinear and soft modes which is removed by a zero-bin subtraction [64]. After this, the remaining UV divergences are removed by multiplicative renormalization counter terms. After UV subtraction and zero-bin subtraction described above, the TMD PDFs or FFs still contain collinear divergence due to the tagged hadron in initial state or final state, and the remaining infrared poles are absorbed into the partonic dimensional regularized collinear PDFs

$$\begin{aligned}
\phi_{ij}(x,\alpha_s) = {} & \delta_{ij}\delta(1-x) - \frac{\alpha_s}{4\pi}\frac{P^{(0)}_{ij}(x)}{\epsilon} \\
& + \left(\frac{\alpha_s}{4\pi}\right)^2 \left[\frac{1}{2\epsilon^2}\left(\sum_k P^{(0)}_{ik}\otimes P^{(0)}_{kj}(x) + \beta_0 P^{(0)}_{ij}(x)\right) - \frac{1}{2\epsilon}P^{(1)}_{ij}(x)\right] \\
& + \left(\frac{\alpha_s}{4\pi}\right)^3 \left[\frac{-1}{6\epsilon^3}\left(\sum_{m,k} P^{(0)}_{im}\otimes P^{(0)}_{mk}\otimes P^{(0)}_{kj}(x) + 3\beta_0\sum_k P^{(0)}_{ik}\otimes P^{(0)}_{kj}(x) + 2\beta_0^2 P^{(0)}_{ij}(x)\right)\right. \\
& + \frac{1}{6\epsilon^2}\left(\sum_k P^{(0)}_{ik}\otimes P^{(1)}_{kj}(x) + 2\sum_k P^{(1)}_{ik}\otimes P^{(0)}_{kj}(x) + 2\beta_0 P^{(1)}_{ij}(x) + 2\beta_1 P^{(0)}_{ij}(x)\right) \\
& \left. - \frac{1}{3\epsilon}P^{(2)}_{ij}(x)\right] + \mathcal{O}(\alpha_s^3)\,,
\end{aligned} \tag{2.8}$$

or the FFs

$$\begin{aligned}
d_{ij}(z,\alpha_s) = {} & \delta_{ij}\delta(1-z) - \frac{\alpha_s}{4\pi}\frac{P^{T(0)}_{ij}(z)}{\epsilon} \\
& + \left(\frac{\alpha_s}{4\pi}\right)^2 \left[\frac{1}{2\epsilon^2}\left(\sum_k P^{T(0)}_{ik}\otimes P^{T(0)}_{kj}(z) + \beta_0 P^{T(0)}_{ij}(z)\right) - \frac{1}{2\epsilon}P^{T(1)}_{ij}(z)\right] \\
& + \left(\frac{\alpha_s}{4\pi}\right)^3 \left[\frac{-1}{6\epsilon^3}\left(\sum_{m,k} P^{T(0)}_{im}\otimes P^{T(0)}_{mk}\otimes P^{T(0)}_{kj}(z) + 3\beta_0\sum_k P^{T(0)}_{ik}\otimes P^{T(0)}_{kj}(z) + 2\beta_0^2 P^{T(0)}_{ij}(z)\right)\right. \\
& + \frac{1}{6\epsilon^2}\left(2\sum_k P^{T(0)}_{ik}\otimes P^{T(1)}_{kj}(z) + \sum_k P^{T(1)}_{ik}\otimes P^{T(0)}_{kj}(z) + 2\beta_0 P^{T(1)}_{ij}(z) + 2\beta_1 P^{T(0)}_{ij}(z)\right) \\
& \left. - \frac{1}{3\epsilon}P^{T(2)}_{ij}(z)\right] + \mathcal{O}(\alpha_s^3)\,,
\end{aligned} \tag{2.9}$$

JHEP06(2021)115

where $P_{ij}^{(n)}$ is the $(n+1)$-loop space-like splitting function [65, 66], which are also known to the same accuracy in a massive environment [67, 68]. $P_{ij}^{T(n)}$ is the $(n+1)$-loop time-like splitting function [50–53], and the symbol $\otimes$ is denoted as the convolution of two functions

$$f(z,\cdots)\otimes g(z,\cdots)\equiv\int_z^1\frac{d\xi}{\xi}\,f(\xi,\cdots)\,g(z/\xi,\cdots)\,. \tag{2.10}$$

The steps above can be summarized as the following collinear factorization formulas

$$\begin{aligned}\frac{1}{Z_i^B}\frac{\mathcal{B}_{i/j}^{\rm bare}(x,b_\perp,\mu,\nu)}{\mathcal{S}_{0\rm b}}&=\sum_k\mathcal{I}_{ik}(x,b_\perp,\mu,\nu)\otimes\phi_{kj}(x,\mu)\,,\\ \frac{1}{Z_i^B}\frac{\mathcal{F}_{j/i}^{\rm bare}(z,b_\perp/z,\mu,\nu)}{\mathcal{S}_{0\rm b}}&=\sum_k d_{jk}(z,\mu)\otimes\mathcal{C}_{ki}(z,b_\perp/z,\mu,\nu)\,.\end{aligned} \tag{2.11}$$

where $\mathcal{B}_{i/j}^{\rm bare}$ ($\mathcal{F}_{j/i}^{\rm bare}$) and $\mathcal{S}_{0\rm b}(\alpha_s)$ are the bare TMD PDFs (FFs) and bare zero-bin soft function, and Z_i^B (see in section C) are the multiplicative operator renormalization constants for $i=q,g$. All the quantities are expressed in terms of the renormalized strong coupling α_s. The zero-bin soft function is the same as TMD soft function, which is known to N^{3}LO in ref. [69]. Note also that the time-like TMD soft function is identical to the space-like one [70, 71] up to this order, so we have a universal soft function up to $\mathcal{O}(\alpha_s^3)$.

3 N^{3}LO coefficients for unpolarized quark and gluon TMDs

In this section we give our results for coefficient functions $\mathcal{I}_{ij}$ and $\mathcal{C}_{ij}$. We give only a numeric fit to these functions in the paper, but the full analytic expressions can be found in the supplementary material. For TMD FFs, we give the results for $\mathcal{C}_{ij}$ with an argument $b_\perp/z$, which after divided by z^2 are exactly the results in the hadron frame, see eq. (2.7).

3.1 Renormalization group equations

The renormalized coefficient functions obey the following RG equations

$$\begin{aligned}\frac{d}{d\ln\mu}\mathcal{I}_{ji}(x,b_\perp,\mu,\nu)=&\,2\Big[\Gamma_j^{\rm cusp}(\alpha_s(\mu))\ln\frac{\nu}{xP_+}+\gamma_j^B(\alpha_s(\mu))\Big]\mathcal{I}_{ji}(x,b_\perp,\mu,\nu)\\&-2\sum_k\mathcal{I}_{jk}(x,b_\perp,\mu,\nu)\otimes P_{ki}(x,\alpha_s(\mu))\,,\end{aligned} \tag{3.1}$$

$$\begin{aligned}\frac{d}{d\ln\mu}\mathcal{C}_{ij}(z,b_\perp/z,\mu,\nu)=&\,2\Big[\Gamma_j^{\rm cusp}(\alpha_s(\mu))\ln\frac{z\nu}{P_+}+\gamma_j^B(\alpha_s(\mu))\Big]\mathcal{C}_{ij}(z,b_\perp/z,\mu,\nu)\\&-2\sum_k P_{ik}^T(z,\alpha_s(\mu))\otimes\mathcal{C}_{kj}(z,b_\perp/z,\mu,\nu)\,.\end{aligned} \tag{3.2}$$

The rapidity evolution equations are [15, 72]

$$\begin{aligned}\frac{d}{d\ln\nu}\mathcal{I}_{ji}(x,b_\perp,\mu,\nu)&=-2\left[\int_\mu^{b_0/b_T}\frac{d\bar\mu}{\bar\mu}\Gamma_j^{\rm cusp}(\alpha_s(\bar\mu))+\gamma_j^R(\alpha_s(b_0/b_T))\right]\mathcal{I}_{ji}(x,b_\perp,\mu,\nu)\,,\\ \frac{d}{d\ln\nu}\mathcal{C}_{ij}(z,b_\perp/z,\mu,\nu)&=-2\left[\int_\mu^{b_0/b_T}\frac{d\bar\mu}{\bar\mu}\Gamma_j^{\rm cusp}(\alpha_s(\bar\mu))+\gamma_j^R(\alpha_s(b_0/b_T))\right]\mathcal{C}_{ij}(z,b_\perp/z,\mu,\nu)\,.\end{aligned} \tag{3.3}$$

Expanding the perturbative coefficient functions in terms of $\alpha_s/(4\pi)$, the solution to these evolution equations up to $\mathcal{O}(\alpha_s^3)$ reads,

$$
\begin{aligned}
\mathcal{I}_{ji}^{(0)}(x,b_\perp,\mu,\nu) &= \delta_{ji}\delta(1-x)\,,\\
\mathcal{I}_{ji}^{(1)}(x,b_\perp,\mu,\nu) &= \left(-\frac{\Gamma_0^{\text{cusp}}}{2}L_\perp L_Q+\gamma_0^B L_\perp+\gamma_0^R L_Q\right)\delta_{ji}\delta(1-x)-P_{ji}^{(0)}(x)L_\perp+I_{ji}^{(1)}(x)\,,\\
\mathcal{I}_{ji}^{(2)}(x,b_\perp,\mu,\nu) &= \Bigg[\frac{1}{8}\left(-\Gamma_0^{\text{cusp}}L_Q+2\gamma_0^B\right)\left(-\Gamma_0^{\text{cusp}}L_Q+2\gamma_0^B+2\beta_0\right)L_\perp^2\\
&\quad+\left(\left(-\Gamma_0^{\text{cusp}}L_Q+2\gamma_0^B+2\beta_0\right)\frac{\gamma_0^R}{2}L_Q-\frac{\Gamma_1^{\text{cusp}}}{2}L_Q+\gamma_1^B\right)L_\perp\\
&\quad+\frac{(\gamma_0^R)^2}{2}L_Q^2+\gamma_1^R L_Q\Bigg]\delta_{ji}\delta(1-x)+\left(\frac{1}{2}\sum_l P_{jl}^{(0)}\otimes P_{li}^{(0)}(x)\right.\\
&\quad\left.+\frac{P_{ji}^{(0)}(x)}{2}\left(\Gamma_0^{\text{cusp}}L_Q-2\gamma_0^B-\beta_0\right)\right)L_\perp^2+\Bigg[-P_{ji}^{(1)}(x)-P_{ji}^{(0)}(x)\gamma_0^R L_Q\\
&\quad-\sum_l I_{jl}^{(1)}\otimes P_{li}^{(0)}(x)+\left(-\frac{\Gamma_0^{\text{cusp}}}{2}L_Q+\gamma_0^B+\beta_0\right)I_{ji}^{(1)}(x)\Bigg]L_\perp+\gamma_0^R L_Q I_{ji}^{(1)}(x)+I_{ji}^{(2)}(x)\,,\\
\mathcal{I}_{ji}^{(3)}(x,b_\perp,\mu,\nu) &= L_\perp^3\Bigg[\left(\frac{1}{2}\beta_0+\frac{1}{4}\left(2\gamma_0^B-\Gamma_0^{\text{cusp}}L_Q\right)\right)\sum_l P_{jl}^{(0)}\otimes P_{li}^{(0)}(x)\\
&\quad-\frac{1}{6}\sum_{lk}P_{jl}^{(0)}\otimes P_{lk}^{(0)}\otimes P_{ki}^{(0)}(x)+\delta_{ji}\delta(1-x)\left(\frac{1}{6}\beta_0^2\left(2\gamma_0^B-\Gamma_0^{\text{cusp}}L_Q\right)\right.\\
&\quad\left.+\frac{1}{8}\beta_0\left(2\gamma_0^B-\Gamma_0^{\text{cusp}}L_Q\right)^2+\frac{1}{48}\left(2\gamma_0^B-\Gamma_0^{\text{cusp}}L_Q\right)^3\right)\\
&\quad+P_{ji}^{(0)}\left(-\frac{1}{2}\beta_0\left(2\gamma_0^B-\Gamma_0^{\text{cusp}}L_Q\right)-\frac{1}{3}\beta_0^2-\frac{1}{8}\left(2\gamma_0^B-\Gamma_0^{\text{cusp}}L_Q\right)^2\right)\Bigg]\\
&\quad+L_\perp^2\Bigg[\left(-\frac{3}{2}\beta_0-\frac{1}{2}\left(2\gamma_0^B-\Gamma_0^{\text{cusp}}L_Q\right)\right)\sum_l I_{jl}^{(1)}\otimes P_{li}^{(0)}(x)\\
&\quad+\frac{1}{2}\sum_{lk}I_{jl}^{(1)}\otimes P_{lk}^{(0)}\otimes P_{ki}^{(0)}(x)+\frac{1}{2}\sum_l P_{jl}^{(0)}\otimes P_{li}^{(1)}(x)+\frac{1}{2}\sum_l P_{jl}^{(1)}\otimes P_{li}^{(0)}(x)\\
&\quad+P_{ji}^{(0)}(x)\left(-\frac{1}{2}\beta_1-\frac{1}{2}\left(2\gamma_1^B-\Gamma_1^{\text{cusp}}L_Q\right)\right)+\delta_{ji}\delta(1-x)\left(\frac{1}{4}\beta_1\left(2\gamma_0^B-\Gamma_0^{\text{cusp}}L_Q\right)\right.\\
&\quad\left.+\frac{1}{2}\beta_0\left(2\gamma_1^B-\Gamma_1^{\text{cusp}}L_Q\right)+\frac{1}{4}\left(2\gamma_0^B-\Gamma_0^{\text{cusp}}L_Q\right)(2\gamma_1^B-\Gamma_1^{\text{cusp}}L_Q)\right)\\
&\quad+I_{ji}^{(1)}(x)\left(\frac{3}{4}\beta_0\left(2\gamma_0^B-\Gamma_0^{\text{cusp}}L_Q\right)+\beta_0^2+\frac{1}{8}\left(2\gamma_0^B-\Gamma_0^{\text{cusp}}L_Q\right)^2\right)\\
&\quad+P_{ji}^{(1)}(x)\left(-\beta_0-\frac{1}{2}\left(2\gamma_0^B-\Gamma_0^{\text{cusp}}L_Q\right)\right)\Bigg]\\
&\quad+L_\perp\Bigg[-\sum_l I_{jl}^{(1)}\otimes P_{li}^{(1)}(x)-\sum_l I_{jl}^{(2)}\otimes P_{li}^{(0)}(x)-P_{ji}^{(0)}(x)\gamma_1^R L_Q-P_{ji}^{(2)}(x)\\
&\quad+\delta_{ji}\delta(1-x)\left(2\beta_0\gamma_1^R L_Q+\frac{1}{2}\gamma_1^R\left(2\gamma_0^B-\Gamma_0^{\text{cusp}}L_Q\right)L_Q+\frac{1}{2}(2\gamma_2^B-\Gamma_2^{\text{cusp}}L_Q)\right)
\end{aligned}
$$

$$
+I_{ji}^{(1)}(x)\left(\beta_1+\frac{1}{2}\left(2\gamma_1^B-\Gamma_1^{\mathrm{cusp}}L_Q\right)\right)+I_{ji}^{(2)}(x)\left(2\beta_0+\frac{1}{2}\left(2\gamma_0^B-\Gamma_0^{\mathrm{cusp}}L_Q\right)\right)\Bigg]
$$

$$
+\delta_{ji}\delta(1-x)\gamma_2^R L_Q+I_{ji}^{(1)}(x)\gamma_1^R L_Q+I_{ji}^{(3)}(x)\,, \tag{3.4}
$$

where in $\mathcal{I}_{ji}^{(3)}$ we have used $\gamma_0^R=0$ to simplify the expression and $I_{ji}^{(n)}(z)$ are the scale-independent coefficient functions. We have defined

$$
L_\perp=\ln\frac{b_T^2\mu^2}{b_0^2},\quad L_Q=2\ln\frac{x\,P_+}{\nu},\quad L_\nu=\ln\frac{\nu^2}{\mu^2}\,,\quad b_0=2e^{-\gamma_E}\,. \tag{3.5}
$$

Similarly, the solution to the fragmentation coefficient functions are

$$
\mathcal{C}_{ji}^{(0)}(z,b_\perp/z,\mu,\nu)=\delta_{ji}\delta(1-z)\,,
$$

$$
\mathcal{C}_{ji}^{(1)}(z,b_\perp/z,\mu,\nu)=\left(-\frac{\Gamma_0^{\mathrm{cusp}}}{2}L_\perp L_Q+\gamma_0^B L_\perp+\gamma_0^R L_Q\right)\delta_{ji}\delta(1-z)-P_{ji}^{T(0)}(z)L_\perp+C_{ji}^{(1)}(z)\,,
$$

$$
\begin{aligned}
\mathcal{C}_{ji}^{(2)}(z,b_\perp/z,\mu,\nu)=&\Bigg[\frac{1}{8}\left(-\Gamma_0^{\mathrm{cusp}}L_Q+2\gamma_0^B\right)\left(-\Gamma_0^{\mathrm{cusp}}L_Q+2\gamma_0^B+2\beta_0\right)L_\perp^2\\
&+\left(\left(-\Gamma_0^{\mathrm{cusp}}L_Q+2\gamma_0^B+2\beta_0\right)\frac{\gamma_0^R}{2}L_Q-\frac{\Gamma_1^{\mathrm{cusp}}}{2}L_Q+\gamma_1^B\right)L_\perp\\
&+\frac{(\gamma_0^R)^2}{2}L_Q^2+\gamma_1^R L_Q\Bigg]\delta_{ji}\delta(1-z)+\Bigg(\frac{1}{2}\sum_l P_{jl}^{T(0)}\otimes P_{li}^{T(0)}(z)\\
&+\frac{P_{ji}^{T(0)}(z)}{2}\left(\Gamma_0^{\mathrm{cusp}}L_Q-2\gamma_0^B-\beta_0\right)\Bigg)L_\perp^2+\Bigg[-P_{ji}^{T(1)}(z)-P_{ji}^{T(0)}(z)\gamma_0^R L_Q\\
&-\sum_l P_{jl}^{T(0)}\otimes C_{li}^{(1)}(z)+\left(-\frac{\Gamma_0^{\mathrm{cusp}}}{2}L_Q+\gamma_0^B+\beta_0\right)C_{ji}^{(1)}(z)\Bigg]L_\perp+\gamma_0^R L_Q C_{ji}^{(1)}(z)+C_{ji}^{(2)}(z)\,,
\end{aligned}
$$

$$
\begin{aligned}
\mathcal{C}_{ji}^{(3)}(z,b_\perp/z,\mu,\nu)=&L_\perp^3\Bigg[\left(\frac{1}{2}\beta_0+\frac{1}{4}\left(2\gamma_0^B-\Gamma_0^{\mathrm{cusp}}L_Q\right)\right)\sum_l P_{jl}^{T(0)}\otimes P_{li}^{T(0)}(z)\\
&-\frac{1}{6}\sum_{lk}P_{jl}^{T(0)}\otimes P_{lk}^{T(0)}\otimes P_{ki}^{T(0)}(z)+\delta_{ji}\delta(1-z)\Bigg(\frac{1}{6}\beta_0^2\left(2\gamma_0^B-\Gamma_0^{\mathrm{cusp}}L_Q\right)\\
&+\frac{1}{8}\beta_0\left(2\gamma_0^B-\Gamma_0^{\mathrm{cusp}}L_Q\right)^2+\frac{1}{48}\left(2\gamma_0^B-\Gamma_0^{\mathrm{cusp}}L_Q\right)^3\Bigg)\\
&+P_{ji}^{T(0)}\left(-\frac{1}{2}\beta_0\left(2\gamma_0^B-\Gamma_0^{\mathrm{cusp}}L_Q\right)-\frac{1}{3}\beta_0^2-\frac{1}{8}\left(2\gamma_0^B-\Gamma_0^{\mathrm{cusp}}L_Q\right)^2\right)\Bigg]\\
&+L_\perp^2\Bigg[\left(-\frac{3}{2}\beta_0-\frac{1}{2}\left(2\gamma_0^B-\Gamma_0^{\mathrm{cusp}}L_Q\right)\right)\sum_l P_{jl}^{T(0)}\otimes C_{li}^{(1)}(z)\\
&+\frac{1}{2}\sum_{lk}P_{jl}^{T(0)}\otimes P_{lk}^{T(0)}\otimes C_{ki}^{(1)}(z)+\frac{1}{2}\sum_l P_{jl}^{T(0)}\otimes P_{li}^{T(1)}(z)+\frac{1}{2}\sum_l P_{jl}^{T(1)}\otimes P_{li}^{T(0)}(z)\\
&+P_{ji}^{T(0)}(z)\left(-\frac{1}{2}\beta_1-\frac{1}{2}\left(2\gamma_1^B-\Gamma_1^{\mathrm{cusp}}L_Q\right)\right)+\delta_{ji}\delta(1-z)\Bigg(\frac{1}{4}\beta_1\left(2\gamma_0^B-\Gamma_0^{\mathrm{cusp}}L_Q\right)\\
&+\frac{1}{2}\beta_0\left(2\gamma_1^B-\Gamma_1^{\mathrm{cusp}}L_Q\right)+\frac{1}{4}\left(2\gamma_0^B-\Gamma_0^{\mathrm{cusp}}L_Q\right)\left(2\gamma_1^B-\Gamma_1^{\mathrm{cusp}}L_Q\right)\Bigg)\\
&+C_{ji}^{(1)}(z)\left(\frac{3}{4}\beta_0\left(2\gamma_0^B-\Gamma_0^{\mathrm{cusp}}L_Q\right)+\beta_0^2+\frac{1}{8}\left(2\gamma_0^B-\Gamma_0^{\mathrm{cusp}}L_Q\right)^2\right)
\end{aligned}
$$

$$
\begin{aligned}
&+P_{ji}^{T(1)}(z)\left(-\beta_0-\frac{1}{2}\left(2\gamma_0^B-\Gamma_0^{\text{cusp}}L_Q\right)\right)\Bigg]\\
&+L_\perp\Bigg[-\sum_l P_{jl}^{T(1)}\otimes C_{li}^{(1)}(z)-\sum_l P_{jl}^{T(0)}\otimes C_{li}^{(2)}(z)-P_{ji}^{T(0)}(z)\gamma_1^R L_Q-P_{ji}^{T(2)}(z)\\
&+\delta_{ji}\delta(1-z)\left(2\beta_0\gamma_1^R L_Q+\frac{1}{2}\gamma_1^R\left(2\gamma_0^B-\Gamma_0^{\text{cusp}}L_Q\right)L_Q+\frac{1}{2}(2\gamma_2^B-\Gamma_2^{\text{cusp}}L_Q)\right)\\
&+C_{ji}^{(1)}(z)\left(\beta_1+\frac{1}{2}\left(2\gamma_1^B-\Gamma_1^{\text{cusp}}L_Q\right)\right)+C_{ji}^{(2)}(z)\left(2\beta_0+\frac{1}{2}\left(2\gamma_0^B-\Gamma_0^{\text{cusp}}L_Q\right)\right)\Bigg]\\
&+\delta_{ji}\delta(1-z)\gamma_2^R L_Q+C_{ji}^{(1)}(z)\gamma_1^R L_Q+C_{ji}^{(3)}(z)\,.
\end{aligned}
\tag{3.6}
$$

We stress again that due to the chosen argument, the expressions given above are for TMD FFs in the hadron frame. The anomalous dimensions appeared above are identical to those in space-like case and we have suppressed their dependence on the exact flavor. The logarithms appeared in the fragmentation coefficient functions are defined as

$$
L_\perp=\ln\frac{b_T^2\mu^2}{b_0^2},\quad L_Q=2\ln\frac{P_+}{z\,\nu},\quad L_\nu=\ln\frac{\nu^2}{\mu^2}\,,\quad b_0=2e^{-\gamma_E}\,,
\tag{3.7}
$$

which differ from thsoe in eq. (3.5) only in L_Q. Both space-like and time-like coefficient functions depend on the rapidity regulator being used. Rapidity-regulator-independent TMD PDFs and TMD FFs can be obtained by multiplying the coefficient functions with the squared root of the TMD soft functions $\mathcal{S}(b_\perp,\mu,\nu)$ [26, 27]

$$
\begin{aligned}
f_{\perp,ij}(x,b_\perp,\mu)&=\mathcal{I}_{ij}(x,b_\perp,\mu,\nu)\sqrt{\mathcal{S}(b_\perp,\mu,\nu)}\,,\\
g_{\perp,ij}(z,b_\perp/z,\mu)&=\mathcal{C}_{ij}(z,b_\perp/z,\mu,\nu)\sqrt{\mathcal{S}(b_\perp,\mu,\nu)}\,.
\end{aligned}
\tag{3.8}
$$

3.2 Numerical fits of the N3LO coefficients

The analytic expressions for the coefficient functions will be provided in the supplementary material attached to this paper. In this section we will present their numerical fits.

The coefficient functions develop end-point divergences both in the threshold and high energy limit. We first present here the results for leading threshold limit. The results for high energy limit will be discussed in next section. In the $z\to 1$ limit, we have

$$
\lim_{z\to1}\mathcal{I}_{ij}^{(2)}(z)=\lim_{z\to1}\mathcal{C}_{ji}^{(2)}(z)=\frac{2\gamma_{1,i}^R}{(1-z)_+}\delta_{ij}\,,\quad \lim_{z\to1}\mathcal{I}_{ij}^{(3)}(z)=\lim_{z\to1}\mathcal{C}_{ji}^{(3)}(z)=\frac{2\gamma_{2,i}^R}{(1-z)_+}\delta_{ij}\,,
\tag{3.9}
$$

where $\gamma_{1(2)}^R$ are the two(three)-loop rapidity anomalous dimensions [69, 73]. The relation between threshold limit and rapidity anomalous dimension has been anticipated in [25, 74, 75]. The explicit expressions up to three-loop read [47]

$$
\begin{aligned}
\mathcal{I}_{qq}^{(1)}(z) &= \mathcal{C}_{qq}^{(1)}(z) = 0\,,\\
\mathcal{I}_{qq}^{(2)}(z) &= \mathcal{C}_{qq}^{(2)}(z) = \frac{1}{(1-z)_+}\left[\left(28\zeta_3 - \frac{808}{27}\right)C_A C_F + \frac{224}{27}C_F N_f T_F\right],\\
\mathcal{I}_{qq}^{(3)}(z) &= \mathcal{C}_{qq}^{(3)}(z) = \frac{1}{(1-z)_+}\left[\left(-\frac{1648\zeta_2}{81} - \frac{1808\zeta_3}{27} + \frac{40\zeta_4}{3} + \frac{125252}{729}\right)C_A C_F N_f T_F\right.\\
&\quad + \left(-\frac{176}{3}\zeta_3\zeta_2 + \frac{6392\zeta_2}{81} + \frac{12328\zeta_3}{27} + \frac{154\zeta_4}{3} - 192\zeta_5 - \frac{297029}{729}\right)C_A^2 C_F\\
&\quad \left. + \left(-\frac{608\zeta_3}{9} - 32\zeta_4 + \frac{3422}{27}\right)C_F^2 N_f T_F + \left(-\frac{128}{9}\zeta_3 - \frac{7424}{729}\right)C_F N_f^2 T_F^2\right].
\end{aligned}
\tag{3.10}
$$

We also found that threshold limit exhibits Casimir scaling up to three loops ($n = 1, 2, 3$),

$$
\lim_{z\to 1}\frac{\mathcal{I}_{gg}^{(n)}(z)}{\mathcal{I}_{qq}^{(n)}(z)} = \lim_{z\to 1}\frac{\mathcal{C}_{gg}^{(n)}(z)}{\mathcal{C}_{qq}^{(n)}(z)} = \frac{C_A}{C_F}\,. \tag{3.11}
$$

3.2.1 Numerical fit for TMD PDFs

The analytic expressions of three-loop coefficient functions contain harmonic polylogarithms up to transcendental weight 5. To facilitate straightforward numerical implementation, we provide a numerical fitting to all the coefficient functions. Following ref. [76], we use the following elementary functions to fit the results,

$$
L_x \equiv \ln x\,,\; L_{\bar{x}} \equiv \ln(1-x)\,,\; \bar{x} \equiv 1 - x\,. \tag{3.12}
$$

For two loop and three loop coefficient functions, we fit the exact results in the region $10^{-6} < x < 1 - 10^{-6}$ (Numerical evaluation of HPLs are made with the `HPL` package [77]), and we have set the color factor to numerical values in QCD, i.e.

$$
C_F = \frac{4}{3}\,, \qquad C_A = 3\,, \qquad T_F = \frac{1}{2}\,. \tag{3.13}
$$

In more detail, we subtract the $x \to 0$ and $x \to 1$ limits up to next-to-next-to-leading power (x^1 and $(1-x)^1$). Then we fit the remaining terms in the region $10^{-6} < x < 1 - 10^{-6}$. Combining the two parts, the fitted results can achieve an accuracy better than 10^{-3} for $0 < x < 1$. We show below the numerical fitting with six significant digits. The full numerical fitting is provided as supplementary material attached to this paper. The one loop scale independent coefficient functions are given by

$$
I_{qq}^{(1)}(x) = 2.66667\bar{x}\,, \tag{3.14a}
$$

$$
I_{qg}^{(1)}(x) = 2x\,\bar{x}\,, \tag{3.14b}
$$

$$
I_{gq}^{(1)}(x) = 2.66667x\,, \tag{3.14c}
$$

$$
I_{gg}^{(1)}(x) = 0\,, \tag{3.14d}
$$

The two-loop scale independent coefficient function are given by

$$I_{qq'}^{(2)}(x) = \frac{2.64517}{x} - 4.56035 + x^3\left(-0.0170296L_x^3 - 0.143469L_x^2 + 1.21562L_x - 3.60403\right)$$
$$+ x^2(0.000306717L_x^3 - 1.77306L_x^2 + 5.65477L_x + 3.57046)$$
$$+ x\left(0.444444L_x^3 - 0.666667L_x^2 - 5.33333L_x + 1.89369\right) + 0.444444L_x^3$$
$$- 0.666667L_x^2 + 2.66667L_x - 0.00131644x^5 + 0.0563783x^4 + 1.33333\bar{x}\,, \tag{3.15a}$$

$$I_{q\bar{q}}^{(2)}(x) = I_{qq'}^{(2)}(x) + x^3\left(23.8756L_x^3 - 68.5281L_x^2 + 391.31L_x - 479.112\right)$$
$$+ x^2(1.73989L_x^3 + 29.5744L_x^2 + 207.751L_x + 533.913)$$
$$+ x\left(-0.148148L_x^3 - 0.888889L_x^2 - 1.33333L_x + 6.98894\right) + 0.148148L_x^3$$
$$- 1.33333L_x + 1.66959x^5 - 60.5553x^4 - 0.444444\bar{x} - 2.90423\,, \tag{3.15b}$$

$$I_{qq}^{(2)}(x) = I_{qq'}^{(2)}(x) + (5.53086N_f + 14.9267)\frac{1}{(\bar{x})_+}$$
$$+ N_f\Big\{x^3\left(-0.0532042L_x^2 + 1.92031L_x - 4.39249\right)$$
$$+ x^2\left(0.939547L_x^2 + 3.50359L_x + 1.65854\right)$$
$$+ x\left(0.444444L_x^2 + 1.48148L_x + 2.36991\right) + 0.444444L_x^2 + 1.48148L_x$$
$$+ 0.0178399x^5 - 0.246399x^4 + 4.24691\bar{x} - 7.90123\Big\} + x^3(3.49597L_x^3 - 18.6432L_x^2$$
$$+ 60.163L_x - 48.6244) + x^2\left(-2.49636L_x^3 - 11.0306L_x^2 - 7.51243L_x + 59.7912\right)$$
$$+ (\bar{x})^3\left(3.19726L_{\bar{x}} - 1.32635L_{\bar{x}}^2\right) - 7.11111L_{\bar{x}}^2 + (\bar{x})^2\left(13.4628L_{\bar{x}} - 2.37726L_{\bar{x}}^2\right)$$
$$+ 22.2222L_{\bar{x}} + \bar{x}\left(3.55556L_{\bar{x}}^2 - 17.7778L_{\bar{x}} - 0.105144\right)$$
$$+ x\left(-0.740741L_x^3 - 10.L_x^2 - 11.5556L_x + 1.87655\right)$$
$$- 0.740741L_x^3 - 2.L_x^2 - 8.L_x + 0.070919x^5 - 2.2589x^4 - 10.2974\,, \tag{3.15c}$$

$$I_{qg}^{(2)}(x) = -52.3982 + 0.555556L_{\bar{x}}^3 + (\bar{x})^3\left(-2.91634L_{\bar{x}}^3 + 2.52056L_{\bar{x}}^2 - 54.8176L_{\bar{x}}\right)$$
$$+ (\bar{x})^2\left(0.982654L_{\bar{x}}^3 + 2.72223L_{\bar{x}}^2 - 15.0644L_{\bar{x}}\right) - 1.66667L_{\bar{x}} + \bar{x}(-1.11111L_{\bar{x}}^3$$
$$-4.66667L_{\bar{x}}^2 + 5.L_{\bar{x}} + 58.9092) + x\left(2.44444L_x^3 + 11.6667L_x^2 + 6.66667L_x - 53.6197\right)$$
$$+ 0.777778L_x^3 - 1.16667L_x^2 + 11.3333L_x + 4.0827x^5 - 16.7693x^4$$
$$+ \frac{5.95164}{x} + x^3\left(-0.5403L_x^3 + 15.2935L_x^2 + 21.5425L_x - 103.137\right)$$
$$+ x^2(-1.00863L_x^3 - 20.4656L_x^2 - 24.7319L_x + 200.419)\,, \tag{3.15d}$$

$$
\begin{aligned}
I_{gq}^{(2)}(x) = N_f \Big\{ &- 25.4815 + \bar{x}^3 \left(0.319337 L_{\bar{x}}^2 + 3.6769 L_{\bar{x}}\right) + \bar{x}^2 \left(1.83746 L_{\bar{x}}^2 + 6.59938 L_{\bar{x}}\right) \\
&+ 0.888889 L_{\bar{x}}^2 + 1.18519 L_{\bar{x}} + \bar{x} \left(0.888889 L_{\bar{x}}^2 + 4.74074 L_{\bar{x}} + 8.49383\right) \\
&- 0.0201765 x^6 - 0.0606673 x^5 - 0.710953 x^4 + 10.7761 x^3 - 25.0013 x^2 + 32.0047 x \\
&+ \frac{11.0617}{x} \Big\} + 25.1431 + x^3 \left(2.72767 L_x^3 + 11.0188 L_x^2 + 67.724 L_x + 124.821\right) \\
&+ x^2 \left(0.001443 L_x^3 + 0.195266 L_x^2 + 2.68862 L_x - 86.22\right) \\
&+ x \left(-3.25926 L_x^3 + 9.33333 L_x^2 - 39.1111 L_x + 48.9377\right) - 4.14815 L_x^3 \\
&+ 12.4444 L_x^2 - 66.6667 L_x + \bar{x}^3 \left(8.67537 L_{\bar{x}}^3 - 26.9743 L_{\bar{x}}^2 + 101.276 L_{\bar{x}}\right) \\
&+ \bar{x}^2 \left(-2.72739 L_{\bar{x}}^3 - 25.4335 L_{\bar{x}}^2 - 43.8567 L_{\bar{x}}\right) - 1.48148 L_{\bar{x}}^3 - 4.88889 L_{\bar{x}}^2 \\
&- 20.4444 L_{\bar{x}} + \bar{x} \left(-1.48148 L_{\bar{x}}^3 - 21.7778 L_{\bar{x}}^2 - 41.7778 L_{\bar{x}} - 68.9101\right) \\
&- 1.2442 x^6 + 7.84991 x^5 - 72.9318 x^4 - \frac{44.3476}{x} ,
\end{aligned} \tag{3.15e}
$$

$$
\begin{aligned}
I_{gg}^{(2)}(x) = N_f \Big\{ &12.4444 \frac{1}{(\bar{x})_+} + 0.888889 L_x^3 + 6. L_x^2 + 24.6667 L_x \\
&+ x \left(0.888889 L_x^3 + 3.33333 L_x^2 + 22.6667 L_x + 36.\right) - 2. L_{\bar{x}} \\
&+ \bar{x} \left(2. L_{\bar{x}} + 54.2222\right) - 29.1111 x^2 + \frac{25.1111}{x} - 48.4444 \Big\} + 33.585 \frac{1}{(\bar{x})_+} \\
&- 85.3465 + x^3 \left(-51.5131 L_x^3 + 433.575 L_x^2 - 477.56 L_x + 2429.\right) \\
&+ x^2 \left(-4.94833 L_x^3 - 97.5448 L_x^2 - 706.464 L_x - 1749.4\right) \\
&+ x \left(-24. L_x^3 - 33. L_x^2 - 269. L_x + 221.873\right) - 12. L_x^3 + 3. L_x^2 - 293. L_x \\
&+ \bar{x}^3 \left(4.98201 L_{\bar{x}} - 3.11742 L_{\bar{x}}^2\right) + \bar{x}^2 \left(-67.425 L_{\bar{x}}^2 - 16.306 L_{\bar{x}}\right) - 36. L_{\bar{x}}^2 + 6. L_{\bar{x}} \\
&+ \bar{x} \left(18. L_{\bar{x}}^2 - 6. L_{\bar{x}} - 352.048\right) - 23.039 x^6 + 160.219 x^5 - 756.676 x^4 - \frac{99.7822}{x} .
\end{aligned} \tag{3.15f}
$$

To present the three-loop scale independent coefficient functions, we first perform the following decompositions,

$$
\begin{aligned}
I_{qq'}^{(3)}(x) &= I_{qq'}^{*}(x) + \frac{d^{ABC} d_{ABC}}{32 N_c} I_{d33}(x), \\
I_{q\bar{q}'}^{(3)}(x) &= I_{qq'}^{*}(x) - \frac{d^{ABC} d_{ABC}}{32 N_c} I_{d33}(x), \\
I_{qq}^{(3)}(x) &= I_{qq}^{*}(x) + I_{qq'}^{(3)}(x), \\
I_{q\bar{q}}^{(3)}(x) &= C_F \left(C_A - 2 C_F\right) I_{q\bar{q}}^{*}(x) + I_{q\bar{q}'}^{(3)}(x) ,
\end{aligned} \tag{3.16}
$$

where

$$
d^{ABC} d_{ABC} = 4 \mathrm{Tr}[T^A \{T^B, T^C\}] \mathrm{Tr}[T^A \{T^B, T^C\}] = \frac{(N_c^2 - 1)(N_c^2 - 4)}{N_c} = \frac{40}{3} . \tag{3.17}
$$

The numerical fitting of different color structures are given by

$$
\begin{aligned}
I^*_{qq'}(x) = N_f\Big\{ &-50.3634 + x^3\left(0.117123L_x^4 - 0.314883L_x^3 + 3.53761L_x^2 - 10.541L_x + 18.5347\right)\\
&+ x^2(-0.0026012L_x^4 + 0.703183L_x^3 + 0.199736L_x^2 + 5.14781L_x\\
&- 24.9854) + (\bar{x})^3\left(-0.227266L_{\bar{x}}^3 - 0.0305807L_{\bar{x}}^2 - 3.18523L_{\bar{x}}\right)\\
&+ (\bar{x})^2\left(-0.000912305L_{\bar{x}}^3 + 0.865032L_{\bar{x}}^2 + 1.85446L_{\bar{x}}\right) + \bar{x}(-0.0987654L_{\bar{x}}^3\\
&- 0.493827L_{\bar{x}}^2 - 4.21399L_{\bar{x}} - 8.73525) + x(-0.246914L_x^4 - 1.61317L_x^3\\
&- 8.77153L_x^2 - 12.0035L_x + 51.7382) - 0.246914L_x^4 - 1.61317L_x^3 - 10.5493L_x^2\\
&- 30.9665L_x + 0.102137x^5 - 0.909082x^4 + \frac{5.88282}{x}\Big\} + 307.912 + x^3(1.80474L_x^5\\
&+ 1.58169L_x^4 + 92.844L_x^3 + 24.4101L_x^2 + 724.086L_x + 168.701) + x^2(\\
&- 0.00854607L_x^5 - 4.88703L_x^4 - 33.0209L_x^3 + 188.744L_x^2 - 49.3191L_x\\
&+ 147.078) + (\bar{x})^3\left(-2.52551L_{\bar{x}}^4 + 13.1597L_{\bar{x}}^3 - 119.84L_{\bar{x}}^2 + 333.889L_{\bar{x}}\right)\\
&+ (\bar{x})^2\left(0.0720812L_{\bar{x}}^4 + 1.43763L_{\bar{x}}^3 + 24.7149L_{\bar{x}}^2 + 192.782L_{\bar{x}}\right)\\
&+ \bar{x}(0.246914L_{\bar{x}}^4 + 0.54321L_{\bar{x}}^3 + 6.03113L_{\bar{x}}^2 + 38.031L_{\bar{x}} + 123.709)\\
&+ x\left(1.27407L_x^5 + 2.34568L_x^4 + 4.50092L_x^3 - 70.7153L_x^2 - 270.973L_x + 167.376\right)\\
&- 0.592593L_x^5 + 6.79012L_x^4 - 46.4127L_x^3 + 86.421L_x^2\\
&- 470.887L_x + \frac{-78.9847L_x - 466.384}{x} + 10.7916x^5 - 335.475x^4\,,
\end{aligned}
\tag{3.18a}
$$

$$
\begin{aligned}
I_{d33}(x) = 32.\Big\{ &- x^3\left(-19156.8L_x^5 + 199731.L_x^4 - 2.18614\times10^6L_x^3 + 1.2083\times10^7L_x^2\right.\\
&\left.- 4.5734\times10^7L_x + 7.52147\times10^7\right) - (\bar{x})^3\left(1023.79L_{\bar{x}}^2 + 121.796L_{\bar{x}}\right)\\
&- (\bar{x})^2\left(-93.2504L_{\bar{x}}^2 - 876.881L_{\bar{x}}\right) - \bar{x}\left(0.0241557L_{\bar{x}}^2 - 0.278902L_{\bar{x}} - 0.582336\right)\\
&- x\left(-1.64493L_x^3 + 3.75242L_x^2 + 0.397826L_x - 774.514\right) - 0.0333333L_x^5\\
&+ 0.0833333L_x^4 - 0.132844L_x^3 - 0.339443L_x^2 - 12.6418L_x + 8847.28x^5\\
&- 729429.x^4 - 13.0667 - x^2\left(-538.817L_x^5 - 25014.2L_x^4 - 500678.L_x^3 - 5.37744\right.\\
&\left.\times10^6L_x^2 - 3.09137\times10^7L_x - 7.59345\times10^7\right)\Big\}\,,
\end{aligned}
\tag{3.18b}
$$

$$
\begin{aligned}
I^*_{qq}(x) =& \left(-9.09324N_f^2 + 154.257N_f + 140.136\right)\frac{1}{(\bar{x})_+}\\
&+ N_f^2\Big\{x^3\left(0.666009L_x^3 - 4.08064L_x^2 + 13.5087L_x - 13.4503\right)\\
&+ x^2\left(-0.610414L_x^3 - 2.30736L_x^2 + 0.622374L_x + 20.7035\right) + x(- 0.329218L_x^3\\
&- 0.855967L_x^2 - 1.18519L_x - 6.71567) - 0.329218L_x^3 - 2.43621L_x^2\\
&- 5.66255L_x - 0.000436414x^5 - 0.405417x^4 - 14.1598\bar{x} + 15.8093\Big\}\\
&+ N_f\Big\{x^3\left(-11.0536L_x^4 + 57.1168L_x^3 - 406.207L_x^2 + 1183.43L_x - 2303.63\right)\\
&+ x^2(3.38122L_x^4 + 37.927L_x^3 + 212.612L_x^2 + 982.488L_x + 2012.66)\\
&+ 2.107L_{\bar{x}}^3 + (\bar{x})^3\left(0.189723L_{\bar{x}}^3 + 1.80938L_{\bar{x}}^2 - 2.62339L_{\bar{x}}\right)\\
&+ 10.3704L_{\bar{x}}^2 + (\bar{x})^2\left(0.69507L_{\bar{x}}^3 + 5.12831L_{\bar{x}}^2 - 15.0284L_{\bar{x}}\right)\\
&- 10.4458L_{\bar{x}} + \bar{x}(- 1.0535L_{\bar{x}}^3 - 7.60494L_{\bar{x}}^2 + 48.0993L_{\bar{x}} + 439.611)\\
&+ x\left(0.855967L_x^4 + 12.6639L_x^3 + 16.4326L_x^2 + 43.9956L_x + 164.293\right) + 0.855967L_x^4\\
&+ 11.9396L_x^3 + 59.1809L_x^2 + 187.752L_x - 1.34066x^5 + 82.5779x^4 - 312.745\Big\}\\
&+ x^3(15.3681L_x^5 - 12.7492L_x^4 + 195.91L_x^3 + 1220.54L_x^2 - 4589.86L_x + 14892.1)\\
&+ x^2(- 2.96846L_x^5 - 62.4209L_x^4 - 385.992L_x^3 - 2295.84L_x^2 - 8061.05L_x\\
&- 14175.7) - 34.7654L_{\bar{x}}^3 + (\bar{x})^3\left(-9.48494L_{\bar{x}}^3 - 52.1748L_{\bar{x}}^2 + 111.502L_{\bar{x}}\right)\\
&- 5.09037L_{\bar{x}}^2 + (\bar{x})^2\left(-11.021L_{\bar{x}}^3 - 85.3807L_{\bar{x}}^2 + 413.664L_{\bar{x}}\right)\\
&+ 637.843L_{\bar{x}} + \bar{x}(- 7.90123L_{\bar{x}}^3 + 9.5085L_{\bar{x}}^2 - 487.943L_{\bar{x}} - 2438.69)\\
&+ x\left(-0.301235L_x^5 - 13.037L_x^4 - 60.4295L_x^3 + 90.2398L_x^2 + 400.357L_x + 265.017\right)\\
&- 0.301235L_x^5 - 8.69136L_x^4 - 69.1867L_x^3 - 286.991L_x^2\\
&- 913.865L_x + 9.73661x^5 - 868.539x^4 + 1033.69\,,
\end{aligned}
\tag{3.18c}
$$

$$
\begin{aligned}
I^*_{q\bar{q}}(x) \;=\; & \frac{9N_f}{4}\Big\{x^3\left(-37.3313L_x^4+69.5328L_x^3-1189.55L_x^2+2193.6L_x-4962.46\right)\\
&+x^2(-0.0538545L_x^4+8.68065L_x^3+179.886L_x^2+1428.28L_x+4299.55)\\
&+0.101532\,(\bar{x})^3\,L_{\bar{x}}+0.0172219\,(\bar{x})^2\,L_{\bar{x}}+\bar{x}\,(0.395062L_{\bar{x}}+0.460905)\\
&+x\left(0.131687L_x^4+0.877915L_x^3+4.86623L_x^2+11.488L_x-9.51143\right)\\
&-0.131687L_x^4-0.943759L_x^3-3.41767L_x^2-4.49137L_x-16.6625x^5\\
&+688.059x^4+1.02498\Big\}+\frac{9}{4}\Big\{x^3(-1385.38L_x^5+15741.4L_x^4-165914.L_x^3\\
&+944859.L_x^2-3.53957\times10^6L_x+5.88567\times10^6)+x^2(-42.7578L_x^5\\
&-1977.89L_x^4-39497.9L_x^3-422824.L_x^2-2.42091\times10^6L_x-5.92341\\
&\times10^6)+3.3635\,(\bar{x})^3\,L_{\bar{x}}-1.78893\,(\bar{x})^2\,L_{\bar{x}}+\bar{x}\,(-4.98979L_{\bar{x}}-13.046)\\
&+x\left(0.0148148L_x^5-1.48148L_x^4-13.6105L_x^3-83.3483L_x^2-64.0087L_x+105.151\right)\\
&-0.0148148L_x^5+1.08642L_x^4+10.911L_x^3+17.5783L_x^2\\
&+6.83186L_x-246.269x^5+37870.3x^4+15.737\Big\},
\end{aligned}
\tag{3.18d}
$$

$$
\begin{aligned}
I_{qg}^{(3)}(x) \;=\;& N_f\Big\{532.389 \\
&+ x^3\Big(3.23607L_x^5 - 4.68217L_x^4 + 120.483L_x^3 - 119.874L_x^2 + 453.908L_x + 442.25\Big) \\
&+x^2\Big(-0.0565211L_x^5 - 3.10462L_x^4 - 20.1426L_x^3 - 202.066L_x^2 - 561.287L_x + 424.055\Big) \\
&- 0.154321L_{\bar{x}}^4 - 0.823045L_{\bar{x}}^3 \\
&+ (\bar{x})^3\Big(2.61221L_{\bar{x}}^4 - 9.9784L_{\bar{x}}^3 + 116.968L_{\bar{x}}^2 - 267.94L_{\bar{x}}\Big) + 1.48131L_{\bar{x}}^2 \\
&+ (\bar{x})^2\Big(-0.378008L_{\bar{x}}^4 - 4.9419L_{\bar{x}}^3 - 38.9532L_{\bar{x}}^2 - 203.044L_{\bar{x}}\Big) + 22.2518L_{\bar{x}} \\
&+ \bar{x}(0.308642L_{\bar{x}}^4 + 2.38683L_{\bar{x}}^3 + 3.85219L_{\bar{x}}^2 - 18.9149L_{\bar{x}} - 275.431) + x(\\
&- 0.355556L_x^5 - 3.65432L_x^4 - 21.6379L_x^3 - 75.7833L_x^2 - 71.9808L_x \\
&- 1040.7) + 0.177778L_x^5 + 1.2716L_x^4 + 14.2634L_x^3 + 67.2339L_x^2 \\
&+ 216.898L_x - 2.00607x^5 - 287.428x^4 + \frac{11.9546}{x}\Big\} - 3636.55 \\
&+ x^3\Big(-259.099L_x^5 + 3952.96L_x^4 - 34085.L_x^3 + 221224.L_x^2 - 768027.L_x + 594756.\Big) \\
&+ x^2\Big(-10.1315L_x^5 - 463.996L_x^4 - 8964.71L_x^3 - 91774.6L_x^2 - 536653.L_x + 96171.9\Big) \\
&- 0.925926L_{\bar{x}}^5 + 2.36111L_{\bar{x}}^4 + 14.151L_{\bar{x}}^3 \\
&+ (\bar{x})^3\Big(-264.815L_{\bar{x}}^5 + 1791.21L_{\bar{x}}^4 - 23536.1L_{\bar{x}}^3 + 107809.L_{\bar{x}}^2 - 431667.L_{\bar{x}}\Big) \\
&- 34.2113L_{\bar{x}}^2 \\
&+ (\bar{x})^2\Big(-5.38358L_{\bar{x}}^5 - 180.755L_{\bar{x}}^4 - 3771.6L_{\bar{x}}^3 - 43136.2L_{\bar{x}}^2 - 262007.L_{\bar{x}}\Big) \\
&- 103.526L_{\bar{x}} \\
&+ \bar{x}\Big(1.85185L_{\bar{x}}^5 + 1.08025L_{\bar{x}}^4 - 37.8328L_{\bar{x}}^3 - 107.055L_{\bar{x}}^2 + 85.0903L_{\bar{x}} + 2491.42\Big) \\
&+ x(10.2642L_x^5 + 65.8827L_x^4 + 175.497L_x^3 - 49.2838L_x^2 - 1754.58L_x \\
&- 692466.) - 1.98519L_x^5 + 5.08025L_x^4 - 171.088L_x^3 - 103.238L_x^2 \\
&- 2331.02L_x + \frac{-177.716L_x - 1109.28}{x} + 1274.6x^5 + 4328.89x^4\,,
\end{aligned} \tag{3.18e}
$$

$$
\begin{aligned}
I_{qg}^{(3)}(x) = N_f^2 \biggl\{ & 61.0677 + \bar{x}^3 \Bigl(1.29041 L_{\bar{x}}^3 - 10.4998 L_{\bar{x}}^2 + 27.9136 L_{\bar{x}}\Bigr) \\
& + \bar{x}^2 \Bigl(-1.87711 L_{\bar{x}}^3 - 7.79618 L_{\bar{x}}^2 - 4.36051 L_{\bar{x}}\Bigr) - 0.987654 L_{\bar{x}}^3 - 4.34568 L_{\bar{x}}^2 - 8.2963 L_{\bar{x}} \\
& + \bar{x} \Bigl(-0.987654 L_{\bar{x}}^3 - 5.53086 L_{\bar{x}}^2 - 12.2469 L_{\bar{x}} - 13.2448\Bigr) + 0.0202177 x^6 + 0.107642 x^5 \\
& + 0.828892 x^4 + 21.886 x^3 - 26.2477 x^2 - 44.418 x - \frac{27.2797}{x} \biggr\} + N_f \biggl\{ - 617.49 \\
& + x^3 \Bigl(208.859 L_x^5 + 10.557 L_x^4 + 8704.26 L_x^3 + 1416.74 L_x^2 + 43827.5 L_x + 34568.\Bigr) \\
& + x^2 \Bigl(-2.85131 L_x^5 - 105.472 L_x^4 - 1575.99 L_x^3 - 11432.7 L_x^2 - 36449.3 L_x + 31014.7\Bigr) \\
& + x \Bigl(0.474074 L_x^5 + 1.11934 L_x^4 + 25.2949 L_x^3 - 8.30824 L_x^2 + 333.065 L_x - 28583.3\Bigr) \\
& - 0.948148 L_x^5 - 2.83128 L_x^4 - 39.4623 L_x^3 - 104.954 L_x^2 - 206.825 L_x \\
& + \frac{66.855 L_x + 299.169}{x} + \bar{x}^3 \Bigl(197.15 L_{\bar{x}}^4 - 535.653 L_{\bar{x}}^3 + 8354.24 L_{\bar{x}}^2 - 17173.5 L_{\bar{x}}\Bigr) \\
& + \bar{x}^2 \Bigl(1.34535 L_{\bar{x}}^4 - 64.5016 L_{\bar{x}}^3 - 1685.89 L_{\bar{x}}^2 - 12486. L_{\bar{x}}\Bigr) \\
& + 2.88066 L_{\bar{x}}^4 + 28.3567 L_{\bar{x}}^3 + 127.182 L_{\bar{x}}^2 + 392.738 L_{\bar{x}} \\
& + \bar{x} \Bigl(2.88066 L_{\bar{x}}^4 + 48.3073 L_{\bar{x}}^3 + 198.787 L_{\bar{x}}^2 + 471.463 L_{\bar{x}} + 467.691\Bigr) \\
& - 147.604 x^6 + 1147.94 x^5 - 37319.1 x^4 \biggr\} - 5656.94 \\
& + x^3 \Bigl(304.814 L_x^5 + 710.583 L_x^4 + 16404.3 L_x^3 + 6246.83 L_x^2 + 151636. L_x + 35826.5\Bigr) \\
& + x^2 \Bigl(-0.756674 L_x^5 - 25.0335 L_x^4 - 244.749 L_x^3 + 596.718 L_x^2 + 20659.8 L_x + 30141.2\Bigr) \\
& + x \Bigl(-13.949 L_x^5 + 3.72016 L_x^4 - 169.304 L_x^3 + 1422.91 L_x^2 + 285.265 L_x + 20018.4\Bigr) \\
& + 10.5877 L_x^5 - 58.7654 L_x^4 + 890.817 L_x^3 - 1109.35 L_x^2 \\
& + 10247.7 L_x + \frac{923.18 L_x^2 + 2860.53 L_x + 9121.84}{x} \\
& + \bar{x}^3 \Bigl(89.4404 L_{\bar{x}}^5 + 121.323 L_{\bar{x}}^4 + 3663.99 L_{\bar{x}}^3 - 409.556 L_{\bar{x}}^2 + 32059. L_{\bar{x}}\Bigr) \\
& + \bar{x}^2 \Bigl(-5.31508 L_{\bar{x}}^5 - 114.333 L_{\bar{x}}^4 - 990.403 L_{\bar{x}}^3 - 3650.08 L_{\bar{x}}^2 - 4439.25 L_{\bar{x}}\Bigr) \\
& - 2.46914 L_{\bar{x}}^5 - 30.5761 L_{\bar{x}}^4 - 210.131 L_{\bar{x}}^3 - 843.608 L_{\bar{x}}^2 - 2040.62 L_{\bar{x}} \\
& + \bar{x} \Bigl(-2.46914 L_{\bar{x}}^5 - 58.3951 L_{\bar{x}}^4 - 435.152 L_{\bar{x}}^3 - 1600.97 L_{\bar{x}}^2 - 3150.68 L_{\bar{x}} - 1728.79\Bigr) \\
& - 348.194 x^6 + 3445.64 x^5 - 94871.7 x^4 \,,
\end{aligned}
\tag{3.18f}
$$

$$
\begin{aligned}
I_{gg}^{(3)}(x) = &-6265.65x^6 + 66758.4x^5 - 1.06264\times 10^6 x^4 \\
&+ \Big(378.83L_x^5 + 24477.3L_x^4 + 63961.5L_x^3 + 546586.L_x^2 + 910511.L_x + 495749.\Big)\, x^3 \\
&+ \Big(57.2841L_x^5 + 1945.83L_x^4 + 27126.6L_x^3 + 189429.L_x^2 + 615133.L_x + 439670.\Big)\, x^2 \\
&+ \Big(-100.8L_x^5 - 496.L_x^4 - 1570.17L_x^3 + 7123.33L_x^2 + 13857.3L_x + 19813.6\Big)\, x \\
&+ 28.8L_x^5 - 62.L_x^4 + 3055.28L_x^3 - 176.L_{\bar{x}}^3 + 2488.89L_x^2 \\
&- 839.824L_{\bar{x}}^2 + \Big\{ - 0.0357895x^6 + 0.0966543x^5 - 4.13448x^4 \\
&+ \Big(0.13079L_x^4 - 0.38099L_x^3 + 4.56176L_x^2 - 9.74592L_x + 21.6304\Big)\, x^3 \\
&+ \Big(-0.00273785L_x^4 - 0.619734L_x^3 - 2.15326L_x^2 - 20.9999L_x + 148.982\Big)\, x^2 \\
&+ \Big(0.0987654L_x^4 - 1.61317L_x^3 - 25.3847L_x^2 - 155.483L_x - 118.21\Big)\, x \\
&+ 0.0987654L_x^4 - 1.21811L_x^3 - 19.2242L_x^2 + 0.888889L_{\bar{x}}^2 - 20.4598\frac{1}{(\bar{x})_+} \\
&- 102.721L_x + 6.22222L_{\bar{x}} + \bar{x}^2\Big(0.000979432L_{\bar{x}}^3 + 1.21259L_{\bar{x}}^2 - 8.48683L_{\bar{x}}\Big) \\
&+ \bar{x}\Big(0.197531L_{\bar{x}}^3 - 3.2716L_{\bar{x}}^2 - 17.8909L_{\bar{x}} - 121.663\Big) \\
&+ \bar{x}^3\Big(0.438091L_{\bar{x}}^3 + 0.29313L_{\bar{x}}^2 + 0.409493L_{\bar{x}}\Big) \\
&+ 41.2796 - \frac{60.5749}{x}\Big\} N_f^2 + 315.306\left[\frac{1}{\bar{x}}\right]_+ + 44694.L_x \\
&+ 1142.11L_{\bar{x}} + \bar{x}^2\Big(-231.508L_{\bar{x}}^3 - 499.573L_{\bar{x}}^2 + 11535.3L_{\bar{x}}\Big) \\
&+ \bar{x}\Big(-200.L_{\bar{x}}^3 - 3.56745L_{\bar{x}}^2 - 10.1778L_{\bar{x}} - 23676.7\Big) \\
&+ \bar{x}^3\Big(2652.95L_{\bar{x}}^3 - 969.004L_{\bar{x}}^2 + 51848.5L_{\bar{x}}\Big) \\
&+ \Big\{ - 65.3387x^6 + 1878.62x^5 - 64513.2x^4 \\
&+ \Big(426.686L_x^5 + 47.588L_x^4 + 19161.8L_x^3 - 7284.34L_x^2 + 136127.L_x + 25910.7\Big)\, x^3 \\
&+ \Big(-4.21446L_x^5 - 150.199L_x^4 - 2113.28L_x^3 - 13513.L_x^2 - 27711.8L_x + 22497.\Big)\, x^2 \\
&+ \Big(5.67407L_x^5 + 50.2346L_x^4 + 377.276L_x^3 + 915.648L_x^2 + 274.685L_x + 22082.4\Big)\, x \\
&- 3.79259L_x^5 - 19.358L_x^4 - 254.888L_x^3 + 10.6667L_{\bar{x}}^3 - 1313.87L_x^2 \\
&+ 64.5363L_{\bar{x}}^2 + 347.079\frac{1}{(\bar{x})_+} - 3835.18L_x - 43.8845L_{\bar{x}} \\
&+ \bar{x}^3\Big(-83.5926L_{\bar{x}}^4 + 181.9L_{\bar{x}}^3 - 3263.87L_{\bar{x}}^2 + 6458.66L_{\bar{x}}\Big) \\
&+ \bar{x}\Big(-0.493827L_{\bar{x}}^4 - 3.45679L_{\bar{x}}^3 + 14.1101L_{\bar{x}}^2 + 470.287L_{\bar{x}} + 4782.37\Big) \\
&+ \bar{x}^2\Big(1.57238L_{\bar{x}}^4 + 69.5168L_{\bar{x}}^3 + 968.989L_{\bar{x}}^2 + 5625.16L_{\bar{x}}\Big) - 9860.15 \\
&+ \frac{176.957L_x + 788.476}{x}\Big\} N_f + 31575.9 + \frac{2077.15L_x^2 + 7128.59L_x + 23355.4}{x}\,.
\end{aligned}
\tag{3.18g}
$$

3.2.2 Numerical fit for TMD FFs

Following the same approach, we give in this subsection the results for TMD FFs. The one-loop scale-independent coefficient functions are given by

$$C_{qq}^{(1)}(z) = z^3\,(6.88266L_z - 7.0063 9) + z^2\,(10.467L_z - 0.842818) + z\,(5.33333L_z + 5.33121) \\ + 5.33333L_z + 8.\bar{z} - 0.128696z^6 + 0.818297z^5 - 3.44742z^4 - 5.33333\,, \tag{3.19a}$$

$$C_{gq}^{(1)}(z) = \frac{10.6667L_z}{z} - 10.6667L_z + z\,(5.33333L_z - 5.33333) - 8.\bar{z} + 8.\,, \tag{3.19b}$$

$$C_{qg}^{(1)}(z) = z\,(2. - 4.L_z) + z^2\,(4.L_z - 2.) + 2.L_z\,, \tag{3.19c}$$

$$C_{gg}^{(1)}(z) = -12. + z^3\,(15.486L_z - 15.8938) + z^2\,(-0.449268L_z - 1.89634) \\ - 24.L_z + \frac{24.L_z}{z} - 0.289566z^6 + 1.84117z^5 - 7.7567z^4 + 12.\bar{z} \\ + z\,(48.L_z + 11.9952)\,. \tag{3.19d}$$

The two-loop scale-independent coefficient functions are given by

$$C_{qq}^{(2)}(z) = C_{q'q}^{(2)}(z) + N_f\Big\{5.53086\frac{1}{(\bar{x})_+} + z^3\left(1.70397L_z^2 - 4.64799L_z + 10.359\right) \\ + z^2\left(0.881779L_z^2 - 8.99257L_z - 0.401235\right) \\ + z\left(0.444444L_z^2 - 0.888889L_z - 3.55556\right) + 0.444444L_z^2 \\ - 8.L_z - 1.67901\bar{z} - 0.00933333z^6 + 0.104686z^5 - 1.16427z^4 - 1.97531\Big\} \\ + 14.9267\frac{1}{(\bar{x})_+} + \bar{z}^3\left(3.93463L_{\bar{z}} - 0.760825L_{\bar{z}}^2\right) + \bar{z}^2\left(2.42655L_{\bar{z}}^2 - 12.8657L_{\bar{z}}\right) \\ + 7.11111L_{\bar{z}}^2 - 22.2222L_{\bar{z}} + \bar{z}\left(-3.55556L_{\bar{z}}^2 + 47.1111L_{\bar{z}} + 139.708\right) \\ + z^3\left(-9.26406L_z^3 - 52.8068L_z^2 + 31.8935L_z - 175.006\right) \\ + z^2\left(-22.9319L_z^3 - 1.84413L_z^2 - 1.58947L_z + 42.8001\right) \\ + z\left(-5.18519L_z^3 + 6.L_z^2 - 122.654L_z + 146.514\right) - 5.18519L_z^3 - 14.4444L_z^2 \\ + 75.5681L_z + 0.720394z^6 - 7.22814z^5 + 85.3763z^4 - 260.245\,, \tag{3.20a}$$

$$C_{\bar{q}'q}^{(2)}(z) = C_{q'q}^{(2)}(z)\,, \tag{3.20b}$$

$$C_{\bar{q}q}^{(2)}(z) = C_{q'q}^{(2)}(z) + z^2\left(-1.2533L_z^3 + 26.1088L_z^2 + 241.727L_z + 645.84\right) \\ + z\left(1.33333L_z^3 + 0.888889L_z^2 - 1.33333L_z + 18.5241\right) - 1.33333L_z^3 \\ - 3.55556L_z^2 - 8.44444L_z - 0.444444\bar{z} - 1.48376z^6 + 20.64z^5 - 282.996z^4 \\ - 10.8899 + z^3\left(47.853L_z^3 - 13.7843L_z^2 + 664.436L_z - 389.634\right)\,, \tag{3.20c}$$

$$
\begin{aligned}
C^{(2)}_{q'q}(z) = {} & -48.773 + z^3\left(0.0245052L_z^3 + 0.125079L_z^2 - 1.08241L_z + 3.45972\right) \\
& + z^2\left(0.000177368L_z^3 - 5.32882L_z^2 - 5.58902L_z + 11.417\right) \\
& + z\left(4.88889L_z^3 - 7.33333L_z^2 - 18.6667L_z + 35.4396\right) + 4.88889L_z^3 \\
& - 7.33333L_z^2 - 48.L_z + \frac{7.11111L_z^2 + 3.55556L_z - 1.45999}{z} \\
& + 1.33333\bar{z} - 0.000213858z^6 + 0.00372439z^5 - 0.0868925z^4\,,
\end{aligned} \tag{3.20d}
$$

$$
\begin{aligned}
C^{(2)}_{gq}(z) = {} & 1290.49 + \bar{z}^3\left(-3.84057L_{\bar{z}}^3 + 37.6298L_{\bar{z}}^2 - 86.9353L_{\bar{z}}\right) \\
& + \bar{z}^2\left(2.86982L_{\bar{z}}^3 + 23.1076L_{\bar{z}}^2 - 66.3682L_{\bar{z}}\right) + 1.48148L_{\bar{z}}^3 - 4.44444L_{\bar{z}}^2 \\
& - 48.3094L_{\bar{z}} + \bar{z}\left(1.48148L_{\bar{z}}^3 + 21.3333L_{\bar{z}}^2 - 33.1982L_{\bar{z}} - 441.625\right) \\
& + z^3\left(-5.92385L_z^3 - 22.5299L_z^2 - 110.802L_z + 15.1969\right) \\
& + z^2\left(-0.212249L_z^3 - 5.70494L_z^2 - 67.3286L_z + 304.102\right) \\
& + z\left(-89.1852L_z^3 + 84.8889L_z^2 + 151.253L_z - 1484.97\right) - 45.6296L_z^3 \\
& + 21.3333L_z^2 + 357.939L_z + \frac{-106.667L_z^3 - 282.667L_z^2 + 156.728L_z - 152.722}{z} \\
& - 0.587738z^6 - 3.60247z^5 + 53.0513z^4\,,
\end{aligned} \tag{3.20e}
$$

$$
\begin{aligned}
C^{(2)}_{qg}(z) = {} & -33.5701 + N_f\Big\{\bar{z}^3\left(2.042L_{\bar{z}} - 0.179298L_{\bar{z}}^2\right) + \bar{z}^2\left(0.670481L_{\bar{z}}^2 + 0.602593L_{\bar{z}}\right) \\
& + 0.333333L_{\bar{z}}^2 + 1.11111L_{\bar{z}} + \bar{z}\left(-0.666667L_{\bar{z}}^2 - 1.55556L_{\bar{z}} + 4.87603\right) \\
& + z^3\left(-0.179321L_z^2 + 2.04201L_z + 0.514002\right) \\
& + z^2\left(0.670483L_z^2 - 8.28627L_z - 2.88119\right) \\
& + z\left(-0.666667L_z^2 + 7.33333L_z + 7.50775\right) + 0.333333L_z^2 - 3.33333L_z - 0.015025z^6 \\
& + 0.0450704z^5 - 0.294577z^4 - 6.09183\Big\} + \bar{z}^3\left(3.18953L_{\bar{z}}^3 - 3.71065L_{\bar{z}}^2 + 13.5993L_{\bar{z}}\right) \\
& + \bar{z}^2\left(-1.01091L_{\bar{z}}^3 - 5.20986L_{\bar{z}}^2 + 41.8832L_{\bar{z}}\right) - 0.555556L_{\bar{z}}^3 - 3.5L_{\bar{z}}^2 \\
& + 1.78267L_{\bar{z}} + \bar{z}\left(1.11111L_{\bar{z}}^3 + 8.33333L_{\bar{z}}^2 - 17.232L_{\bar{z}} - 79.1583\right) \\
& + z^3\left(-6.58896L_z^3 - 12.6016L_z^2 - 148.67L_z + 226.183\right) \\
& + z^2\left(-9.99409L_z^3 - 45.4536L_z^2 - 32.8022L_z - 189.651\right) \\
& + z\left(66.8889L_z^3 + 2.66667L_z^2 - 147.41L_z - 10.8933\right) + 8.55556L_z^3 - 24.3333L_z^2 \\
& - 97.2949L_z + \frac{16.L_z^2 + 8.L_z - 3.28497}{z} - 0.7087z^6 - 0.502913z^5 + 33.3265z^4\,,
\end{aligned} \tag{3.20f}
$$

$$
\begin{aligned}
C_{gg}^{(2)}(z) = N_f \Bigg\{ & 12.4444 \frac{1}{(\bar{x})_+} - 127.778\ - 0.000223065 \bar{z}^3 L_{\bar{z}} - 0.0000208355 \bar{z}^2 L_{\bar{z}} \\
& + 2.L_{\bar{z}} + z^3 \left(1.76728 L_z^3 - 4.55758 L_z^2 + 15.8982 L_z + 0.643843\right) \\
& + z^2 \left(0.0299539 L_z^3 + 7.78684 L_z^2 - 25.7082 L_z + 49.0399\right) \\
& + z \left(9.77778 L_z^3 - 19.3333 L_z^2 - 78.L_z + 83.3332\right) + 9.77778 L_z^3 + 7.33333 L_z^2 - 50.L_z \\
& + \frac{-0.888889 L_z^2 - 27.1111 L_z + 3.4321}{z} + 37.5556 \bar{z} - 0.00782998 z^6 + 0.153818 z^5 \\
& - 3.92838 z^4 \Bigg\} + 33.585 \frac{1}{(\bar{x})_+} + 1795.49\ + \bar{z}^3 \left(0.0225989 L_{\bar{z}}^2 + 287.323 L_{\bar{z}}\right) \\
& + \bar{z}^2 \left(66.3821 L_{\bar{z}}^2 + 5.53377 L_{\bar{z}}\right) + 36.L_{\bar{z}}^2 - 6.L_{\bar{z}} + \bar{z} \left(-18.L_{\bar{z}}^2 + 216.L_{\bar{z}} + 444.823\right) \\
& + z^3 \left(-967.096 L_z^3 - 103.327 L_z^2 - 11404.1 L_z + 4605.87\right) \\
& + z^2 \left(-21.4751 L_z^3 - 591.494 L_z^2 - 3594.61 L_z - 9731.14\right) \\
& + z \left(-744.L_z^3 - 75.L_z^2 + 357.518 L_z - 2387.27\right) - 132.L_z^3 + 33.L_z^2 + 1292.74 L_z \\
& + \frac{-240.L_z^3 - 660.L_z^2 + 62.259 L_z - 296.958}{z} + 24.3517 z^6 - 407.965 z^5 + 5728.73 z^4\,.
\end{aligned} \tag{3.20g}
$$

The three-loop scale-independent coefficient functions are given by

$$
\begin{aligned}
C_{qq}^{(3)}(z) = C_{q'q}^{(3)}(z) + N_f\Big\{ & 154.257\frac{1}{(\bar{x})_+} + \bar{z}^3\left(1.03702L_{\bar{z}}^3 + 0.00482051L_{\bar{z}}^2 - 1.98623L_{\bar{z}}\right) \\
& + \bar{z}^2\left(-0.691297L_{\bar{z}}^3 - 5.00561L_{\bar{z}}^2 - 0.834261L_{\bar{z}}\right) - 2.107L_{\bar{z}}^3 - 10.3704L_{\bar{z}}^2 \\
& + 13.8356L_{\bar{z}} + \bar{z}\left(1.0535L_{\bar{z}}^3 - 3.55556L_{\bar{z}}^2 - 26.922L_{\bar{z}} + 57.6679\right) \\
& + z^3\left(-19.7036L_z^4 + 33.1654L_z^3 - 444.349L_z^2 + 661.632L_z - 1870.9\right) \\
& + z^2\left(-1.9698L_z^4 + 30.6275L_z^3 + 191.742L_z^2 + 337.809L_z + 2071.18\right) \\
& + z\left(-0.148148L_z^4 - 12.0933L_z^3 + 50.6066L_z^2 + 131.174L_z - 355.483\right) \\
& - 0.148148L_z^4 + 4.56516L_z^3 + 115.265L_z^2 - 458.905L_z + 0.5958z^6 \\
& - 10.0011z^5 + 300.139z^4 + 138.622\Big\} + N_f^2\Big\{ - 9.09324\frac{1}{(\bar{x})_+} \\
& + z^3\left(1.13739L_z^3 - 1.11292L_z^2 + 8.49447L_z + 0.132844\right) \\
& + z^2\left(0.911883L_z^3 - 3.47057L_z^2 + 5.15991L_z - 2.6942\right) \\
& + z\left(0.460905L_z^3 - 0.855967L_z^2 - 2.50206L_z - 0.131794\right) + 0.460905L_z^3 \\
& - 2.43621L_z^2 + 8.82305L_z - 7.57543\bar{z} - 0.0139459z^6 + 0.212281z^5 - 3.95786z^4 \\
& + 9.22493\Big\} + 140.136\frac{1}{(\bar{x})_+} + \bar{z}^3\left(144.25L_{\bar{z}}^4 - 566.24L_{\bar{z}}^3 + 6271.93L_{\bar{z}}^2 - 15644.6L_{\bar{z}}\right) \\
& + \bar{z}^2\left(-4.10249L_{\bar{z}}^4 - 121.769L_{\bar{z}}^3 - 1804.41L_{\bar{z}}^2 - 12411.1L_{\bar{z}}\right) + 34.7654L_{\bar{z}}^3 \\
& + 5.09037L_{\bar{z}}^2 - 1826.42L_{\bar{z}} + \bar{z}\left(-42.6667L_{\bar{z}}^3 + 32.8626L_{\bar{z}}^2 + 1865.35L_{\bar{z}} - 104.524\right) \\
& + z^3\left(55.5684L_z^5 + 409.681L_z^4 + 1340.71L_z^3 + 9286.53L_z^2 - 212.8L_z + 19119.9\right) \\
& + z^2\left(12.7948L_z^5 - 7.34615L_z^4 - 652.115L_z^3 - 4213.45L_z^2 - 9887.78L_z + 17171.7\right) \\
& + z\left(0.330864L_z^5 - 14.4444L_z^4 + 235.053L_z^3 - 739.672L_z^2 + 998.485L_z - 22860.2\right) \\
& + 0.330864L_z^5 - 1.73663L_z^4 - 235.432L_z^3 - 1059.64L_z^2 \\
& + 3285.53L_z - 53.6084z^6 + 420.432z^5 - 16201.7z^4 + 133.444\,,
\end{aligned}
\tag{3.21a}
$$

JHEP06(2021)115

$$
\begin{aligned}
C^{(3)}_{\bar{q}q}(z) = C^{(3)}_{\bar{q}'q}(z) + N_f \Big\{ & \bar{z}^3 \left(-10.7901 L_{\bar{z}}^3 - 1.1804 L_{\bar{z}}^2 - 172.111 L_{\bar{z}}\right) \\
& + \bar{z}^2 \left(-0.301929 L_{\bar{z}}^3 - 6.5035 L_{\bar{z}}^2 - 51.1538 L_{\bar{z}}\right) + \bar{z}\,(0.395062 L_{\bar{z}} + 0.460905) \\
& + z^3 \left(-17.0335 L_z^4 - 137.582 L_z^3 - 499.752 L_z^2 - 1860.45 L_z - 759.677\right) \\
& + z^2 \left(-1.91048 L_z^4 - 4.52615 L_z^3 - 95.3246 L_z^2 - 571.103 L_z - 524.745\right) \\
& + z \left(0.773663 L_z^4 - 1.62414 L_z^3 - 7.72423 L_z^2 + 14.3251 L_z - 277.011\right) - 0.773663 L_z^4 \\
& + 1.16324 L_z^3 + 3.64193 L_z^2 + 13.9018 L_z + 15.9632 z^6 - 137.732 z^5 + 1650.43 z^4 \\
& + 32.7672 \Big\} + \bar{z}^3 \left(1380.49 L_{\bar{z}}^4 - 3405.35 L_{\bar{z}}^3 + 54960. L_{\bar{z}}^2 - 107954. L_{\bar{z}}\right) \\
& + \bar{z}^2 \left(-26.476 L_{\bar{z}}^4 - 909.761 L_{\bar{z}}^3 - 12653. L_{\bar{z}}^2 - 84025.1 L_{\bar{z}}\right) + \bar{z}\,(-4.98979 L_{\bar{z}} - 13.046) \\
& + z^3 \left(-486.111 L_z^5 + 2695.54 L_z^4 - 19026.4 L_z^3 + 99236. L_z^2 - 179433. L_z + 137119.\right) \\
& + z^2 \left(15.2308 L_z^5 + 265.21 L_z^4 + 2452.17 L_z^3 + 12096.8 L_z^2 - 16346.8 L_z + 124275.\right) \\
& + z \left(-2.35556 L_z^5 - 14.8148 L_z^4 + 109.379 L_z^3 + 142.666 L_z^2 - 100.216 L_z - 192966.\right) \\
& + 2.35556 L_z^5 + 24.4527 L_z^4 - 16.7701 L_z^3 + 103.935 L_z^2 \\
& + 333.13 L_z - 1141.38 z^6 + 6288.46 z^5 - 73997. z^4 + 422.31\,,
\end{aligned}
\tag{3.21b}
$$

$$
C^{(3)}_{q'q}(z) = C^{*}_{q'q}(z) + \frac{d^{ABC} d_{ABC}}{32 N_c} C_{d33}(z)\,, \tag{3.21c}
$$

$$
C^{(3)}_{\bar{q}'q}(z) = C^{*}_{q'q}(z) - \frac{d^{ABC} d_{ABC}}{32 N_c} C_{d33}(z)\,, \tag{3.21d}
$$

$$
\begin{aligned}
C^{*}_{q'q}(z) = N_f \Big\{ & 27.0915 + \bar{z}^3 \left(0.193659 L_{\bar{z}}^3 + 0.293846 L_{\bar{z}}^2 - 2.24651 L_{\bar{z}}\right) \\
& + \bar{z}^2 \left(0.00288809 L_{\bar{z}}^3 - 1.70852 L_{\bar{z}}^2 - 7.99319 L_{\bar{z}}\right) \\
& + \bar{z} \left(-0.0987654 L_{\bar{z}}^3 - 0.493827 L_{\bar{z}}^2 - 1.28966 L_{\bar{z}} - 3.86138\right) \\
& + z^3 \left(0.151889 L_z^4 + 0.157662 L_z^3 - 0.309824 L_z^2 + 6.09781 L_z + 1.00545\right) \\
& + z^2 \left(-0.00133511 L_z^4 - 3.60493 L_z^3 + 16.2546 L_z^2 - 24.7872 L_z + 12.0106\right) \\
& + z \left(0.790123 L_z^4 - 4.6749 L_z^3 + 23.4989 L_z^2 + 10.1958 L_z - 30.7157\right) \\
& + 0.790123 L_z^4 - 13.5638 L_z^3 - 2.87145 L_z^2 + 11.7244 L_z \\
& + \frac{6.32099 L_z^3 + 4.74074 L_z^2 + 5.47355 L_z - 6.50358}{z} - 0.0100925 z^6 + 0.0433735 z^5 \\
& - 2.92155 z^4 \Big\} + 2356.76 + \bar{z}^3 \left(1.99803 L_{\bar{z}}^4 + 0.201226 L_{\bar{z}}^3 + 60.9292 L_{\bar{z}}^2 + 14.0251 L_{\bar{z}}\right) \\
& + \bar{z}^2 \left(-0.026975 L_{\bar{z}}^4 + 1.5332 L_{\bar{z}}^3 - 1.66342 L_{\bar{z}}^2 - 74.0435 L_{\bar{z}}\right) \\
& + \bar{z} \left(0.246914 L_{\bar{z}}^4 - 0.938272 L_{\bar{z}}^3 - 4.14606 L_{\bar{z}}^2 + 61.3677 L_{\bar{z}} + 90.0722\right) \\
& + z^3 \left(1.44997 L_z^5 + 5.483 L_z^4 + 123.168 L_z^3 + 176.819 L_z^2 + 923.553 L_z + 28.2894\right) \\
& + z^2 \left(-0.00167084 L_z^5 + 22.4717 L_z^4 + 1.00054 L_z^3 - 146.27 L_z^2 + 790.245 L_z + 5.17563\right) \\
& + z \left(-43.2296 L_z^5 + 85.358 L_z^4 - 173.688 L_z^3 - 919.477 L_z^2 + 3982.24 L_z - 2387.44\right) \\
& + 5.03704 L_z^5 - 14.7654 L_z^4 + 79.7975 L_z^3 - 990.195 L_z^2 + 273.338 L_z \\
& + \frac{-54.5185 L_z^4 - 353.975 L_z^3 - 346.753 L_z^2 - 131.107 L_z + 712.406}{z} \\
& - 3.27908 z^6 + 33.6575 z^5 - 745.562 z^4 \,,
\end{aligned} \tag{3.21e}
$$

$$
\begin{aligned}
C_{d33}(z) = \; & \bar{z}^2 \left(-0.307397 L_{\bar{z}}^2 - 38.4701 L_{\bar{z}}\right) + \bar{z} \left(-1.54596 L_{\bar{z}}^2 + 16.3038 L_{\bar{z}} + 62.8465\right) \\
& + z^3 \left(2.97919 L_z^5 + 34.253 L_z^4 + 132.475 L_z^3 + 595.614 L_z^2 + 587.898 L_z + 520.873\right) \\
& + z^2 \left(0.0487062 L_z^5 - 34.2258 L_z^4 + 134.207 L_z^3 + 383.35 L_z^2 + 246.025 L_z + 472.994\right) \\
& + z \left(2.66667 L_z^4 - 260.948 L_z^3 + 967.077 L_z^2 - 1766.62 L_z + 1419.94\right) \\
& + 7.46667 L_z^5 - 6.22222 L_z^4 - 10.3848 L_z^3 + 706.144 L_z^2 + 521.357 L_z + 4.63572 z^6 \\
& - 11.1449 z^5 - 872.326 z^4 - 1534.97 + \bar{z}^3 \left(-0.269815 L_{\bar{z}}^2 - 28.5219 L_{\bar{z}}\right) \,,
\end{aligned} \tag{3.21f}
$$

$$
\begin{aligned}
C^{(3)}_{gq}(z) = N_f\Big\{ & -1108.48 + \bar{z}^3\left(7.58584L_{\bar{z}}^4 - 31.4672L_{\bar{z}}^3 + 228.754L_{\bar{z}}^2 - 476.836L_{\bar{z}}\right)\\
& + \bar{z}^2\left(-0.940842L_{\bar{z}}^4 - 14.0264L_{\bar{z}}^3 - 53.8666L_{\bar{z}}^2 - 174.207L_{\bar{z}}\right)\\
& - 0.411523L_{\bar{z}}^4 - 1.86557L_{\bar{z}}^3 + 31.6117L_{\bar{z}}^2 + 126.856L_{\bar{z}}\\
& + \bar{z}\left(-0.411523L_{\bar{z}}^4 - 6.1454L_{\bar{z}}^3 - 1.90267L_{\bar{z}}^2 + 162.885L_{\bar{z}} + 913.267\right)\\
& + z^3\left(4.57512L_z^5 + 11.1861L_z^4 + 203.498L_z^3 + 290.533L_z^2 + 1265.34L_z + 630.954\right)\\
& + z^2\left(-0.0370741L_z^5 - 1.40262L_z^4 - 28.1512L_z^3 - 174.684L_z^2 - 95.9495L_z + 559.385\right)\\
& + z\left(-4.02963L_z^5 + 6.02469L_z^4 + 24.2085L_z^3 - 459.232L_z^2 + 915.724L_z + 599.07\right)\\
& + 8.05926L_z^5 - 24.4938L_z^4 - 133.619L_z^3 - 1101.17L_z^2 + 1025.8L_z\\
& + \frac{-36.0823L_z^4 - 70.5844L_z^3 - 30.0038L_z^2 - 1644.91L_z + 531.011}{z}\\
& - 3.68167z^6 + 46.0164z^5 - 1188.42z^4\Big\} - 16659.8\\
& + \bar{z}^3\left(35.4193L_{\bar{z}}^5 - 219.487L_{\bar{z}}^4 + 1485.12L_{\bar{z}}^3 - 4170.57L_{\bar{z}}^2 + 10384.9L_{\bar{z}}\right)\\
& + \bar{z}^2\left(-5.35238L_{\bar{z}}^5 - 42.4256L_{\bar{z}}^4 + 5.94854L_{\bar{z}}^3 - 133.051L_{\bar{z}}^2 - 1489.25L_{\bar{z}}\right)\\
& - 2.46914L_{\bar{z}}^5 + 7.94239L_{\bar{z}}^4 + 115.51L_{\bar{z}}^3 - 515.669L_{\bar{z}}^2 - 1954.74L_{\bar{z}}\\
& + \bar{z}\left(-2.46914L_{\bar{z}}^5 - 23.1687L_{\bar{z}}^4 + 119.033L_{\bar{z}}^3 + 1075.92L_{\bar{z}}^2 - 2726.04L_{\bar{z}} - 17725.8\right)\\
& + z^3\left(-76.1738L_z^5 - 9.10623L_z^4 - 2287.06L_z^3 - 7866.64L_z^2 - 5529.82L_z - 18309.8\right)\\
& + z^2\left(0.537045L_z^5 + 45.4989L_z^4 + 819.376L_z^3 + 722.523L_z^2 + 15767.9L_z - 16612.4\right)\\
& + z\left(518.199L_z^5 - 1121.6L_z^4 + 829.631L_z^3 + 21325.1L_z^2 - 33619.9L_z + 29876.3\right)\\
& - 89.9951L_z^5 + 149.728L_z^4 + 1805.41L_z^3 + 20822.L_z^2 - 2827.94L_z\\
& + \frac{384.L_z^5 + 3473.78L_z^4 + 5160.83L_z^3 + 6813.26L_z^2 + 37045.7L_z + 7355.78}{z}\\
& + 49.7303z^6 - 749.182z^5 + 14561.3z^4,
\end{aligned}
\tag{3.21g}
$$

$$
\begin{aligned}
C_{qg}^{(3)}(z) = &-199.178z^6 + 216.114z^5 - 7090.88z^4 \\
&+ \left(-156.025L_z^5 + 166.04L_z^4 - 4677.54L_z^3 + 2353.55L_z^2 - 15669.L_z + 452.173\right) z^3 \\
&+ \left(10.1476L_z^5 + 308.931L_z^4 + 318.491L_z^3 + 6648.7L_z^2 + 38837.8L_z + 74.1398\right) z^2 \\
&+ \left(-395.365L_z^5 - 435.299L_z^4 - 651.612L_z^3 - 873.892L_z^2 + 8857.9L_z - 3975.65\right) z \\
&- 0.925926L_{\bar{z}}^5 + 16.8741L_z^5 - 12.0833L_{\bar{z}}^4 - 25.9012L_z^4 - 54.8189L_{\bar{z}}^3 \\
&- 255.16L_z^3 - 28.4699L_{\bar{z}}^2 - 4389.82L_z^2 + \Big\{ - 0.000633714z^6 + 0.0260241z^5 \\
&- 0.665263z^4 + \left(-0.0765408L_z^3 + 1.70812L_z^2 - 8.03237L_z + 9.12771\right) z^3 \\
&+ \left(1.03454L_z^3 - 5.86883L_z^2 + 7.22527L_z - 4.90518\right) z^2 \\
&+ \left(-1.03704L_z^3 + 5.25926L_z^2 - 4.39289L_z - 9.7382\right) z - 0.37037L_{\bar{z}}^3 + 0.518519L_z^3 \\
&- 1.85185L_{\bar{z}}^2 - 1.85185L_z^2 + 1.26572L_{\bar{z}} + \bar{z}^2 \left(-0.73545L_{\bar{z}}^3 - 1.69507L_{\bar{z}}^2 + 8.70289L_{\bar{z}}\right) \\
&+ \bar{z}^3 \left(0.330843L_{\bar{z}}^3 - 1.24575L_{\bar{z}}^2 + 1.0939L_{\bar{z}}\right) \\
&+ \bar{z} \left(0.740741L_{\bar{z}}^3 + 2.59259L_{\bar{z}}^2 - 7.12403L_{\bar{z}} - 6.15555\right) - 0.0998535L_z + 9.56988\Big\} N_f^2 \\
&+ 275.019L_{\bar{z}} + \bar{z}^2 \left(-2.93658L_{\bar{z}}^5 - 70.6885L_{\bar{z}}^4 - 754.615L_{\bar{z}}^3 - 4257.26L_{\bar{z}}^2 - 13872.4L_{\bar{z}}\right) \\
&+ \bar{z} \left(1.85185L_{\bar{z}}^5 + 28.7346L_{\bar{z}}^4 + 139.144L_{\bar{z}}^3 - 109.864L_{\bar{z}}^2 - 1688.1L_{\bar{z}} - 2655.53\right) \\
&+ \bar{z}^3 \left(88.7527L_{\bar{z}}^5 + 138.689L_{\bar{z}}^4 + 3798.44L_{\bar{z}}^3 + 4087.64L_{\bar{z}}^2 + 17552.1L_{\bar{z}}\right) \\
&+ 1017.76L_z + \Big\{ - 21.5862z^6 + 150.038z^5 - 4826.58z^4 \\
&+ \left(26.6804L_z^5 + 4.22518L_z^4 + 1004.59L_z^3 + 571.353L_z^2 + 4318.31L_z + 5231.6\right) z^3 \\
&+ \left(-0.395692L_z^5 - 18.1614L_z^4 - 227.L_z^3 - 1356.54L_z^2 - 6051.6L_z + 4714.16\right) z^2 \\
&+ \left(3.02222L_z^5 - 8.2716L_z^4 - 63.1193L_z^3 - 254.718L_z^2 + 89.1164L_z - 4904.57\right) z \\
&- 1.51111L_z^5 + 1.08025L_{\bar{z}}^4 + 0.765432L_z^4 + 11.251L_{\bar{z}}^3 \\
&+ 0.806584L_z^3 + 26.1788L_{\bar{z}}^2 + 273.617L_z^2 - 30.318L_{\bar{z}} \\
&+ \bar{z} \left(-2.16049L_{\bar{z}}^4 - 24.428L_{\bar{z}}^3 - 37.4317L_{\bar{z}}^2 + 179.106L_{\bar{z}} + 330.174\right) \\
&+ \bar{z}^2 \left(1.41617L_{\bar{z}}^4 - 0.661483L_{\bar{z}}^3 - 339.004L_{\bar{z}}^2 - 2561.81L_{\bar{z}}\right) \\
&+ \bar{z}^3 \left(34.8293L_{\bar{z}}^4 - 104.9L_{\bar{z}}^3 + 1456.48L_{\bar{z}}^2 - 2987.62L_{\bar{z}}\right) + 99.119L_z \\
&- 424.185 + \frac{13.5638L_z^3 - 9.74486L_z^2 + 1.61518L_z - 10.5514}{z}\Big\} N_f + 9611.66 \\
&+ \frac{-122.667L_z^4 - 814.222L_z^3 - 1026.22L_z^2 - 442.914L_z + 1652.6}{z},
\end{aligned}
\tag{3.21h}
$$

$$
\begin{aligned}
C_{gg}^{(3)}(z) = {}& 13587.6z^6 - 182029.z^5 + 4.31788\times10^6 z^4 + \Big(-17646.9L_z^5 - 32932.7L_z^4 \\
& - 895202.L_z^3 - 506008.L_z^2 - 6.67683\times10^6 L_z - 2.23289\times10^6\Big) z^3 + \Big(111.781L_z^5 \\
& + 4555.84L_z^4 + 63933.2L_z^3 + 367397.L_z^2 + 694258.L_z - 1.99903\times10^6\Big) z^2 \\
& + \Big(4334.4L_z^5 + 2099.L_z^4 + 1739.67L_z^3 + 121402.L_z^2 - 10723.5L_z + 190560.\Big) z \\
& - 244.8L_z^5 + 380.L_z^4 + 176.L_{\bar z}^3 + 3912.39L_z^3 + 839.824L_{\bar z}^2 \\
& + 61497.1L_z^2 + \Big\{ - 0.0586466z^6 - 0.0523985z^5 + 3.93521z^4 \\
& + \Big(-0.853738L_z^4 + 3.18919L_z^3 - 22.3459L_z^2 + 51.4518L_z - 104.039\Big) z^3 \\
& + \Big(0.00929978L_z^4 - 3.60852L_z^3 - 3.74294L_z^2 + 104.196L_z + 35.241\Big) z^2 \\
& + \Big(1.18519L_z^4 - 25.5144L_z^3 + 51.8078L_z^2 + 58.689L_z - 146.248\Big) z \\
& + 1.18519L_z^4 - 27.0947L_z^3 - 0.888889L_{\bar z}^2 + 5.70903L_z^2 - 20.4598\frac{1}{(\bar x)}_+ \\
& - 6.22222L_{\bar z} + \bar z^2\Big(0.00178891L_{\bar z}^3 - 1.13567L_{\bar z}^2 - 2.99102L_{\bar z}\Big) \\
& + \bar z\Big(0.197531L_{\bar z}^3 - 0.604938L_{\bar z}^2 - 16.9247L_{\bar z} - 99.3166\Big) \\
& + \bar z^3\Big(0.618545L_{\bar z}^3 + 1.03642L_{\bar z}^2 - 0.613943L_{\bar z}\Big) + 113.908L_z \\
& + 240.465 + \frac{0.263374L_z^3 + 1.5144L_z^2 + 37.1139L_z - 7.39814}{z}\Big\} N_f^2 \\
& + 315.306\frac{1}{(\bar x)}_+ - 7159.3L_{\bar z} + \bar z^3\Big(-4055.59L_{\bar z}^3 - 2593.37L_{\bar z}^2 - 48610.9L_{\bar z}\Big) \\
& + \bar z\Big(-376.L_{\bar z}^3 - 1179.39L_{\bar z}^2 + 12927.7L_{\bar z} + 3854.88\Big) \\
& + \bar z^2\Big(234.799L_{\bar z}^3 - 891.557L_{\bar z}^2 - 27609.5L_{\bar z}\Big) \\
& - 656.548L_z + \Big\{ - 366.473z^6 + 5156.93z^5 - 148894.z^4 \\
& + \Big(771.541L_z^5 + 751.33L_z^4 + 35545.6L_z^3 + 5384.26L_z^2 + 246456.L_z + 81634.5\Big) z^3 \\
& + \Big(-6.90626L_z^5 - 256.962L_z^4 - 3539.19L_z^3 - 23870.L_z^2 - 52024.3L_z + 71845.1\Big) z^2 \\
& + \Big(-114.03L_z^5 + 344.525L_z^4 + 647.313L_z^3 - 3967.84L_z^2 + 7537.44L_z - 8883.28\Big) z \\
& + 32.237L_z^5 - 60.2469L_z^4 - 10.6667L_{\bar z}^3 - 287.664L_z^3 \\
& - 64.5363L_{\bar z}^2 - 6169.48L_z^2 + 347.079\frac{1}{(\bar x)}_+ + 61.0452L_{\bar z} \\
& + \bar z^2\Big(-1.53589L_{\bar z}^4 - 72.1586L_{\bar z}^3 - 964.26L_{\bar z}^2 - 5462.05L_{\bar z}\Big) \\
& + \bar z\Big(-0.493827L_{\bar z}^4 + 4.24691L_{\bar z}^3 + 66.1118L_{\bar z}^2 + 0.917326L_{\bar z} + 2403.55\Big) \\
& + \bar z^3\Big(96.2988L_{\bar z}^4 - 145.492L_{\bar z}^3 + 3741.37L_{\bar z}^2 - 6474.06L_{\bar z}\Big) - 5069.6L_z + 100.426 \\
& + \frac{-74.0741L_z^4 + 136.494L_z^3 + 909.237L_z^2 - 3714.97L_z + 905.703}{z}\Big\} N_f - 145882. \\
& + \frac{864.L_z^5 + 8008.L_z^4 + 15340.7L_z^3 + 23082.4L_z^2 + 76348.7L_z + 19111.9}{z}\,.
\end{aligned}
\tag{3.21i}
$$

4 Small x expansion of unpolarized TMD coefficients and resummation for TMD FFs

In this section we give the results for TMD PDFs and FFs expanded in high energy limit, namely $x, z \to 0$. A striking difference between space-like TMD PDFs and time-like TMD FFs is that there is only single logarithmic enhancement in each order of perturbative expansion in TMD PDFs, while in TMD FFs it becomes double logarithmic enhancement. We also resum the small-z logarithms in TMD FFs to Next-to-Next-to-Leading Logarithmic (NNLL) accuracy in this section.

4.1 Small-x expansion of unpolarized TMD PDFs

Using the analytic expression we obtained, it is straightforward to obtain the small-x expansion. At leading power in the expansion, the results read

$$\begin{aligned}
xI^{(2)}_{qq}(x) &= xI^{(2)}_{qq'}(x) = xI^{(2)}_{q\bar{q}}(x) = xI^{(2)}_{q\bar{q}'}(x) = 2C_F T_F \left(\frac{172}{27} - \frac{8\zeta_2}{3}\right), \\
xI^{(3)}_{qq}(x) &= xI^{(3)}_{qq'}(x) = xI^{(3)}_{q\bar{q}}(x) = xI^{(3)}_{q\bar{q}'}(x) \\
&= 2T_F \Bigg[\left(\frac{208\zeta_2}{9} + \frac{32\zeta_3}{3} - \frac{17152}{243}\right) C_A C_F \ln x + \left(-16\zeta_2 + \frac{512}{9}\zeta_3 + \frac{32}{3}\zeta_4 - \frac{269}{9}\right) C_F^2 \\
&\quad + \left(\frac{12008\zeta_2}{81} + 120\zeta_3 + \frac{920\zeta_4}{9} - \frac{456266}{729}\right) C_A C_F + \left(-\frac{32\zeta_2}{9} - \frac{64\zeta_3}{9} + \frac{16928}{729}\right) C_F N_f T_F \Bigg].
\end{aligned} \tag{4.1}$$

$$\begin{aligned}
xI^{(2)}_{qg}(x) &= 2C_A T_F \left(\frac{172}{27} - \frac{8\zeta_2}{3}\right), \\
xI^{(3)}_{qg}(x) &= 2T_F \Bigg[\left(\frac{208\zeta_2}{9} + \frac{32\zeta_3}{3} - \frac{17152}{243}\right) C_A^2 \ln x + \left(\frac{160\zeta_2}{27} - \frac{32\zeta_3}{9} - \frac{3164}{729}\right) C_A N_f T_F \\
&\quad + \left(-16\zeta_2 + \frac{512\zeta_3}{9} + \frac{32\zeta_4}{3} - \frac{269}{9}\right) C_A C_F + \left(\frac{12536\zeta_2}{81} + \frac{1096\zeta_3}{9} + \frac{920\zeta_4}{9} - \frac{470494}{729}\right) C_A^2 \\
&\quad + \left(-\frac{512\zeta_2}{27} - \frac{64\zeta_3}{9} + \frac{40184}{729}\right) C_F N_f T_F \Bigg],
\end{aligned} \tag{4.2}$$

$$\begin{aligned}
xI^{(2)}_{gq}(x) &= C_A C_F \left[\frac{88}{3}\zeta_2 + 48\zeta_3 - \frac{3160}{27}\right] + \frac{448}{27} C_F N_f T_F, \\
xI^{(3)}_{gq}(x) &= C_A^2 C_F \Bigg[64\zeta_3 \ln^2 x + \left(-\frac{7504}{27}\zeta_2 - 80\zeta_3 - \frac{392}{3}\zeta_4 + \frac{75584}{81}\right) \ln x \\
&\quad - \frac{103304}{81}\zeta_2 + \frac{320}{3}\zeta_2\zeta_3 - \frac{1504}{3}\zeta_3 - \frac{12436}{9}\zeta_4 - \frac{4208}{3}\zeta_5 + \frac{333613}{54} \Bigg] \\
&\quad + C_A C_F^2 \left[-\frac{512}{3}\zeta_3\zeta_2 + 88\zeta_2 - 672\zeta_3 + 368\zeta_4 + \frac{2432}{3}\zeta_5 - \frac{1105}{6} \right] \\
&\quad + C_A C_F N_f T_F \Bigg[\left(-\frac{512}{27}\zeta_2 + 64\zeta_3 + \frac{1424}{81}\right) \ln x - \frac{2432}{27}\zeta_2 + \frac{832}{9}\zeta_3 + 16\zeta_4 \\
&\quad + \frac{68548}{243} \Bigg] + C_F^3 \left[192\zeta_3\zeta_2 - 104\zeta_2 + 592\zeta_3 - 392\zeta_4 - 640\zeta_5 + \frac{467}{3} \right] \\
&\quad + C_F^2 N_f T_F \Bigg[\left(\frac{1024}{27}\zeta_2 - \frac{128}{3}\zeta_3 - \frac{19040}{243}\right) \ln x + \frac{9776}{81}\zeta_2 - \frac{1696}{9}\zeta_3 - 32\zeta_4 \\
&\quad - \frac{139334}{729} \Bigg] + C_F N_f^2 T_F^2 \left[-\frac{128}{3}\zeta_3 - \frac{7424}{243} \right].
\end{aligned} \tag{4.3}$$

$$
\begin{aligned}
xI_{gg}^{(2)}(x) &= C_A^2\left[\frac{88}{3}\zeta_2+48\zeta_3-\frac{3160}{27}\right]+\frac{484}{27}C_AN_fT_F-\frac{8}{3}C_FN_fT_F\,,\\
xI_{gg}^{(3)}(x) &= C_A^3\left[64\zeta_3\ln^2x+\left(-\frac{7504}{27}\zeta_2-\frac{176}{3}\zeta_3-\frac{392}{3}\zeta_4+\frac{75584}{81}\right)\ln x\right.\\
&\quad\left.-\frac{112928}{81}\zeta_2+128\zeta_2\zeta_3-\frac{1792}{3}\zeta_3-1452\zeta_4-1232\zeta_5+\frac{1572769}{243}\right]\\
&\quad+C_A^2N_fT_F\left[\left(-\frac{512}{27}\zeta_2+\frac{320}{3}\zeta_3+\frac{1568}{81}\right)\ln x-\frac{16288}{81}\zeta_2-\frac{512}{9}\zeta_3\right.\\
&\quad\left.+\frac{1040}{9}\zeta_4+\frac{535048}{729}\right]+C_AC_FN_fT_F\left[\left(\frac{1024}{27}\zeta_2-128\zeta_3-\frac{19904}{243}\right)\ln x\right.\\
&\quad\left.+\frac{10144}{27}\zeta_2+\frac{256\zeta_3}{9}-\frac{1376}{9}\zeta_4-\frac{836194}{729}\right]+C_AN_f^2T_F^2\left[-\frac{128}{9}\zeta_3-\frac{40160}{729}\right]\\
&\quad+C_F^2N_fT_F\left[\frac{160}{9}\zeta_2-\frac{896}{9}\zeta_3+\frac{1024}{9}\zeta_4+12\right]+C_FN_f^2T_F^2\left[\frac{35776}{729}-\frac{512}{9}\zeta_3\right].
\end{aligned}
\tag{4.4}
$$

We note that a LL prediction for the small-x expansion has been given in [78]. After fixing a typo in that paper, we find full agreement with its LL prediction for both quark and gluon TMD PDFs at small x.[1] It would be very interesting to extend the formalism of [78] beyond LL and compare with the data presented here.

4.2 Small-z expansion of unpolarized TMD FFs

To facilitate small-z resummation for TMD FFs, we shall consider the coefficient functions in flavor singlet sector below, since non-singlet TMD FFs are at most logarithmic divergent, but not power divergent in the $z \to 0$ limit. The flavor singlet (denoted by a superscript ^{s}) coefficient functions can be written as a matrix,

$$
\widehat{C}^s(z) = \begin{pmatrix} \widetilde{C}_{qq}(z) & 2N_fC_{qg}(z) \\ C_{gq}(z) & C_{gg}(z) \end{pmatrix}\,, \tag{4.5}
$$

where

$$
\widetilde{C}_{qq}(z) = C_{qq}(z) + C_{\bar{q}q}(z) + (N_f-1)(C_{q'q}(z)+C_{\bar{q}'q}(z))\,, \tag{4.6}
$$

and $C_{ij}(z)$ are scaleless coefficient functions as appeared in the solutions of RG equation (3.6).

In contrast to TMD PDFs, which contribute a single logarithm at each perturbative order in the small-x, TMD FFs in the singlet sector develop small-z double logarithms,

$$
\lim_{z\to 0} z\widehat{C}^s_{kj}(z) = \lim_{z\to 0} z\sum_{n=1}^{\infty} a_s^n \widehat{C}^{s(n)}_{kj}(z) \sim \sum_{n=1}^{\infty} a_s^n\left(\sum_{m=1}^{2n}\ln^{2n-m}z\right), \tag{4.7}
$$

where $a_s = \alpha_s/(4\pi)$ is our perturbative expansion parameter. The small-z data for quark fragmentation in the singlet sector are (non-singlet sector results are suppressed in the

[1] We thank Simone Marzani for communicating with us the typo in eq. (40) of [78].

$z\to 0$ limit)

$$
\begin{aligned}
z\widehat{C}_{qq}^{s(1)}(z) &= 0\,,\\
z\widehat{C}_{qq}^{s(2)}(z) &= 2N_fC_FT_F\left(\frac{32}{3}\ln^2 z+\frac{16}{3}\ln z+\frac{16}{3}\zeta_2-\frac{296}{27}\right),\\
z\widehat{C}_{qq}^{s(3)}(z) &= 2N_fC_AC_FT_F\biggl[-\frac{736}{27}\ln^4 z-\frac{14336}{81}\ln^3 z+\left(-\frac{64}{9}\zeta_2-\frac{14632}{81}\right)\ln^2 z+\biggl(\frac{256}{3}\zeta_3\\
&\quad-\frac{3616}{27}\zeta_2+\frac{11312}{243}\biggr)\ln z-\frac{1472}{9}\zeta_4+112\zeta_3-\frac{17600}{81}\zeta_2+\frac{512156}{729}\biggr]\\
&\quad+2N_fC_F^2T_F\left[\frac{128}{3}\ln^2 z+\left(-128\zeta_3+\frac{128}{9}\zeta_2+\frac{1288}{9}\right)\ln z-\frac{608}{3}\zeta_4+\frac{32}{9}\zeta_3+\frac{6272}{27}\zeta_2\right.\\
&\quad\left.-\frac{1262}{27}\right]+2C_FN_f^2T_F^2\left[\frac{512}{27}\ln^3 z+\frac{128}{9}\ln^2 z+\left(-\frac{256}{9}\zeta_2+\frac{5120}{81}\right)\ln z-\frac{64}{9}\zeta_2-\frac{5696}{729}\right].
\end{aligned}
\tag{4.8}
$$

$$
\begin{aligned}
z\widehat{C}_{gq}^{s(1)}(z) &= 8C_F\ln z\,,\\
z\widehat{C}_{gq}^{s(2)}(z) &= C_AC_F\left[-\frac{80}{3}\ln^3 z-\frac{212}{3}\ln^2 z+(32\zeta_2+12)\ln z-88\zeta_3-\frac{88}{3}\zeta_2+\frac{3128}{27}\right]\\
&\quad+C_F^2\Bigl[(48-64\zeta_2)\ln z\Bigr],\\
z\widehat{C}_{gq}^{s(3)}(z) &= C_A^2C_F\biggl[32\ln^5 z+\frac{7816}{27}\ln^4 z+\left(\frac{7376}{9}-\frac{2560}{9}\zeta_2\right)\ln^3 z+\biggl(-\frac{1984}{3}\zeta_2+\frac{1184}{3}\zeta_3\\
&\quad+\frac{8608}{9}\biggr)\ln^2 z+\left(\frac{3776}{3}\zeta_2+\frac{3136}{3}\zeta_3+1408\zeta_4-\frac{123892}{81}\right)\ln z+\frac{7456\zeta_5}{3}+\frac{608}{3}\zeta_2\zeta_3\\
&\quad+\frac{5870}{3}\zeta_4-\frac{7588}{9}\zeta_3+\frac{21944}{27}\zeta_2-\frac{3650707}{729}\biggr]+C_AC_F^2\biggl[\left(\frac{1792}{9}\zeta_2-\frac{1360}{9}\right)\ln^3 z\\
&\quad+\left(-\frac{64}{3}\zeta_3+\frac{1888}{3}\zeta_2-\frac{1532}{3}\right)\ln^2 z+\left(\frac{488}{3}\zeta_4-\frac{80}{3}\zeta_3-\frac{1360}{3}\zeta_2+\frac{701}{9}\right)\ln z\\
&\quad+\frac{6800}{3}\zeta_5+992\zeta_3\zeta_2+\frac{830}{3}\zeta_4-1746\zeta_3-\frac{48568}{27}\zeta_2+\frac{10141}{9}\biggr]\\
&\quad+C_AC_FN_fT_F\biggl[-\frac{32}{27}\ln^4 z+\frac{3712}{81}\ln^3 z+\left(\frac{896}{9}\zeta_2+\frac{152}{81}\right)\ln^2 z+\biggl(-\frac{320}{3}\zeta_3\\
&\quad-\frac{4384}{27}\zeta_2-\frac{67384}{243}\biggr)\ln z+\frac{688}{9}\zeta_4+\frac{704}{3}\zeta_3+\frac{10864}{81}\zeta_2-\frac{50600}{729}\biggr]\\
&\quad+C_F^3\biggl[\left(\frac{128}{3}\zeta_3-64\zeta_2+\frac{208}{3}\right)\ln^2 z+\left(\frac{1600}{3}\zeta_4-336\zeta_3-\frac{224}{3}\zeta_2-\frac{173}{3}\right)\ln z\\
&\quad-416\zeta_5-\frac{2240}{3}\zeta_3\zeta_2+796\zeta_4+\frac{2888}{3}\zeta_3+608\zeta_2-\frac{4715}{3}\biggr]\\
&\quad+C_F^2N_fT_F\biggl[-\frac{1024}{27}\ln^4 z-\frac{4928}{27}\ln^3 z+\left(-\frac{256}{3}\zeta_2-\frac{7184}{27}\right)\ln^2 z\\
&\quad+\left(-\frac{448}{3}\zeta_3-\frac{1280}{9}\zeta_2+\frac{2060}{27}\right)\ln z-\frac{224}{3}\zeta_4-\frac{1664}{9}\zeta_3-\frac{5984}{27}\zeta_2+\frac{75770}{729}\biggr].
\end{aligned}
\tag{4.9}
$$

$$
\begin{aligned}
z\widehat{C}_{qg}^{s(1)}(z) &= 0\,,\\
z\widehat{C}_{qg}^{s(2)}(z) &= 2N_fC_AT_F\left[\frac{32}{3}\ln^2 z+\frac{16}{3}\ln z+\frac{16}{3}\zeta_2-\frac{296}{27}\right],
\end{aligned}
$$

$$
\begin{aligned}
z\widehat{C}_{qg}^{s(3)}(z) =\, & 2N_f C_A^2 T_F\Bigg[\left(-\frac{832}{9}\zeta_2-\frac{1160}{9}\right)\ln^2 z+\left(-\frac{4640}{27}\zeta_2+\frac{256}{3}\zeta_3+\frac{14360}{243}\right)\ln z \\
& -\frac{736}{27}\ln^4 z-\frac{14656}{81}\ln^3 z-\frac{2368}{27}\zeta_2+\frac{976}{9}\zeta_3-\frac{2432}{9}\zeta_4+\frac{152392}{243}\Bigg] \\
& +2N_f C_A C_F T_F\Bigg[\left(\frac{256}{3}\zeta_2-\frac{64}{3}\right)\ln^2 z+\left(\frac{512}{9}\zeta_2-128\zeta_3+\frac{1000}{9}\right)\ln z \\
& +\frac{3040}{27}\zeta_2+\frac{32}{9}\zeta_3-96\zeta_4+\frac{514}{27}\Bigg]+2C_A N_f^2 T_F^2\Bigg[\left(\frac{1136}{81}-\frac{512}{27}\zeta_2\right)\ln z \\
& +\frac{896}{81}\ln^3 z-\frac{3328}{81}\ln^2 z-\frac{512}{81}\zeta_2-\frac{64}{9}\zeta_3+\frac{256}{27}\Bigg]+2C_F N_f^2 T_F^2\Bigg[\Bigg(\frac{224}{3} \\
& -\frac{512}{27}\zeta_2\Bigg)\ln z+\frac{1280}{81}\ln^3 z+\frac{5120}{81}\ln^2 z-\frac{2048}{81}\zeta_2+\frac{128}{9}\zeta_3+\frac{10304}{729}\Bigg].
\end{aligned} \tag{4.10}
$$

$$
\begin{aligned}
z\widehat{C}_{gg}^{s(1)}(z) =\, & 8C_A\ln z\,, \\
z\widehat{C}_{gg}^{s(2)}(z) =\, & C_A^2\Bigg[\left(\frac{536}{9}-32\zeta_2\right)\ln z-\frac{80}{3}\ln^3 z-\frac{220}{3}\ln^2 z-\frac{88}{3}\zeta_2-88\zeta_3+\frac{3268}{27}\Bigg] \\
& +C_A N_f T_F\Bigg[-\frac{16}{3}\ln^2 z-\frac{184}{9}\ln z+\frac{556}{27}\Bigg]+C_F N_f T_F\Bigg[\frac{32}{3}\ln^2 z+\frac{16}{3}\ln z-\frac{1112}{27}\Bigg], \\
z\widehat{C}_{gg}^{s(3)}(z) =\, & C_A^3\Bigg[\left(\frac{57392}{81}-\frac{256}{3}\zeta_2\right)\ln^3 z+\left(-\frac{352}{3}\zeta_2+416\zeta_3+\frac{14792}{27}\right)\ln^2 z \\
& +\left(\frac{19984}{27}\zeta_2+\frac{5632}{9}\zeta_3+2104\zeta_4-\frac{344864}{243}\right)\ln z+32\ln^5 z+\frac{8008}{27}\ln^4 z \\
& -\frac{34640}{81}\zeta_2+448\zeta_2\zeta_3-\frac{14576}{9}\zeta_3+3256\zeta_4+4336\zeta_5-\frac{1348136}{243}\Bigg] \\
& +C_A^2 N_f T_F\Bigg[\left(\frac{256}{3}\zeta_2+\frac{22816}{81}\right)\ln^2 z+\left(-\frac{3616}{27}\zeta_2+\frac{256}{9}\zeta_3-\frac{46912}{81}\right)\ln z \\
& +\frac{352}{27}\ln^4 z+\frac{5152}{27}\ln^3 z-\frac{3136}{81}\zeta_2+\frac{3152}{9}\zeta_3+240\zeta_4-\frac{230840}{729}\Bigg] \\
& +C_A C_F N_f T_F\Bigg[\left(-\frac{256}{9}\zeta_2-\frac{37072}{81}\right)\ln^2 z+\left(-\frac{3008}{27}\zeta_2-\frac{2560}{9}\zeta_3+\frac{92560}{243}\right)\ln z \\
& -\frac{1792}{27}\ln^4 z-\frac{29248}{81}\ln^3 z+\frac{3856}{27}\zeta_2-\frac{1552}{3}\zeta_3-\frac{8720}{9}\zeta_4+\frac{849464}{729}\Bigg] \\
& +C_A N_f^2 T_F^2\Bigg[\frac{256}{81}\ln^3 z+\frac{1472}{81}\ln^2 z+\frac{3776}{243}\ln z-\frac{128}{9}\zeta_3-\frac{52256}{729}\Bigg] \\
& +C_F^2 N_f T_F\Bigg[\left(\frac{1024}{9}\zeta_3-\frac{352}{3}\right)\ln z+\frac{64}{3}\ln^2 z+\frac{2752}{9}\zeta_3+\frac{832}{3}\zeta_4-\frac{1684}{3}\Bigg] \\
& +C_F N_f^2 T_F^2\Bigg[-\frac{512}{81}\ln^3 z-\frac{2944}{81}\ln^2 z+\frac{18560}{243}\ln z+\frac{256}{9}\zeta_3+\frac{104512}{729}\Bigg].
\end{aligned} \tag{4.11}
$$

We note that while both $\widehat{C}_{qi}^s$ and $\widehat{C}_{gi}^s$ has double logarithmic expansion in the small-z limit, the power of leading logarithmic terms of $\widehat{C}_{qi}^s$ is lower by 1 than the corresponding leading logarithmic terms of $\widehat{C}_{gi}^s$.

4.3 Resummation of small-x logarithms for unpolarized TMD FFs

In this subsection, we shall derive the all-order resummation at NNLL accuracy (resummation of the highest three logarithms) in eq. (4.7), following an idea proposed in [56]. To

JHEP06(2021)115

this end, we begin with the unrenormalized version of collinear factorization formula in eq. (2.11) for singlet TMD FFs (see (4.6) for the definition of singlet combination),

$$\mathcal{F}^s_{i/j}(z,\epsilon) = \frac{1}{Z^B_j}\frac{\mathcal{F}^{s,\mathrm{bare}}_{i/j}(z,\epsilon)}{\mathcal{S}_{0\mathrm{b}}} = \sum_k d^s_{ik}\otimes C^s_{kj}(z,\epsilon)\,, \tag{4.12}$$

where the convolution is in z. Note that $\mathcal{F}^s_{i/j}(z,\epsilon)$ is a quantity to which the usual strong coupling renormalization, zero-bin subtraction and operator renormalization have been performed. However renormalization of collinear FFs has not been performed, which is why we still keep the ϵ dependence in (4.12). From now on we concentrate on the scale-independent part of the coefficient functions by setting all the scale logarithms to zero. We can do this because the scale logarithms depends either on anomalous dimension, which has no z dependence, or on time-like splitting functions, whose small-z behavior is known to NNLL accuracy [57]. It proves convenient to work in Mellin-N space also, which is defined as

$$\mathcal{F}(\overline{N},\epsilon) = M[\mathcal{F}(z,\epsilon)] := \int_0^1 dz\, z^{N-1}\mathcal{F}(z,\epsilon)\,, \tag{4.13}$$

where $\overline{N} = N-1$. Small-z logarithms becomes poles in $\bar{N}$ under Mellin transformation,

$$M\left[\frac{1}{z}\ln^k z\right] \equiv \int_0^1 dz\, z^{N-1}\frac{1}{z}\ln^k z = \frac{(-1)^k k!}{(N-1)^{k+1}} = \frac{(-1)^k k!}{\overline{N}^{k+1}}\,. \tag{4.14}$$

In Mellin space the unrenormalized collinear factorization formula in eq. (4.12) becomes

$$\begin{pmatrix} \mathcal{F}^s_{qi}(\overline{N},\epsilon) \\ \mathcal{F}^s_{gi}(\overline{N},\epsilon) \end{pmatrix} = \widehat{d}^s(\overline{N},\epsilon)\cdot \begin{pmatrix} \widehat{C}^s_{qi}(\overline{N},\epsilon) \\ \widehat{C}^s_{gi}(\overline{N},\epsilon) \end{pmatrix}\,, \tag{4.15}$$

where

$$\widehat{d}^s(\overline{N},\epsilon) = \begin{pmatrix} \widehat{d}^s_{qq}(\overline{N},\epsilon) & \widehat{d}^s_{qg}(\overline{N},\epsilon) \\ \widehat{d}^s_{gq}(\overline{N},\epsilon) & \widehat{d}^s_{gg}(\overline{N},\epsilon) \end{pmatrix}\,. \tag{4.16}$$

The collinear FFs in $\overline{\mathrm{MS}}$ scheme evolve with time-like splitting functions. In Mellin moment space it reads

$$\frac{d}{d\ln\mu^2}\widehat{d}^s(\overline{N},\epsilon) = 2\widehat{d}^s(\overline{N},\epsilon)\cdot\widehat{\gamma}^T(\overline{N})\,, \tag{4.17}$$

where $\widehat{\gamma}^T(\overline{N})$ is the time-like singlet splitting function in Mellin space. Its complete NNLO results can be found in [50], see also [51–53].

The crucial observation of [56] is that unrenormalized collinear functions have specific singular behavior in the limit of small-z in dimensional regularization. In the case of TMD FFs, we can write down an general ansatz at small z,

$$\begin{aligned}
\mathcal{F}^{s(n)}_{g/i}(z,\epsilon) &= \frac{1}{\epsilon^{2n-1}}\sum_{l=0}^{n-1} z^{-1-2(n-l)\epsilon}\Big(\underbrace{c^{(1,l,n)}_{gi}}_{\text{LL}} + \underbrace{\epsilon c^{(2,l,n)}_{gi}}_{\text{NLL}} + \underbrace{\epsilon^2 c^{(3,l,n)}_{gi}}_{\text{NNLL}} + \dots\Big)\,,\\
\mathcal{F}^{s(n)}_{q/i}(z,\epsilon) &= \frac{1}{\epsilon^{2n-2}}\sum_{l=0}^{n-2} z^{-1-2(n-l)\epsilon}\Big(\underbrace{c^{(1,l,n)}_{qi}}_{\text{LL}} + \underbrace{\epsilon c^{(2,l,n)}_{qi}}_{\text{NLL}} + \underbrace{\epsilon^2 c^{(3,l,n)}_{qi}}_{\text{NNLL}} + \dots\Big)\,,
\end{aligned} \tag{4.18}$$

JHEP06(2021)115

where $c_{gi}^{(1,l,n)}$ is the leading term in the ϵ expansion and small-z expansion, whose knowledge correspond to LL resummation as labeled in (4.18), and similarly for other terms. Precisely, for $\widehat{C}_{gi}^{s}(z)$ the LL series correspond to $\alpha_s^n \ln^{2n-1} z$ terms, while NLL correspond to $\alpha_s^n \ln^{2n-2} z$, and NNLL to $\alpha_s^n \ln^{2n-3} z$. For $\widehat{C}_{qi}^{s}(z)$ the corresponding power of $\ln z$ is lower by 1. We have verified this general ansatz through explicit N^{3}LO calculation from its operator definition in (2.6) and (2.7). In Mellin space the corresponding ansatz reads

$$\begin{aligned}
\mathcal{F}_{g/i}^{s(n)}(\overline{N},\epsilon) =& \frac{1}{\epsilon^{2n-1}}\sum_{l=0}^{n-1}\frac{1}{\overline{N}-2(n-l)\epsilon}\left(c_{gi}^{(1,l,n)}+\epsilon c_{gi}^{(2,l,n)}+\epsilon^2 c_{gi}^{(3,l,n)}+\dots\right),\\
\mathcal{F}_{q/i}^{s(n)}(\overline{N},\epsilon) =& \frac{1}{\epsilon^{2n-2}}\sum_{l=0}^{n-2}\frac{1}{\overline{N}-2(n-l)\epsilon}\left(c_{qi}^{(1,l,n)}+\epsilon c_{qi}^{(2,l,n)}+\epsilon^2 c_{qi}^{(3,l,n)}+\dots\right).
\end{aligned} \tag{4.19}$$

Equations (4.18) or (4.19) provides a way to resum all the large logarithms of z. Specifically, if one knows all the $c_{gi}^{1,l,n}$ for all l and n, then one can do LL resummation for $\mathcal{F}_{g/i}^{s}$, and similarly for NLL and NNLL resummation. In this paper instead of working out the constants for all n, we provide results for n up to 15, which is sufficient for phenomenological purpose.

We note that the neglected terms in (4.19) are higher orders in ϵ and in $\overline{N}$. To facilitate easy extraction of the constants, it is convenient to define a “small-z” weight:

$$[\overline{N}] = 1\,, \qquad [\epsilon] = 1\,, \qquad [\text{numbers}] = 0\,, \tag{4.20}$$

such that $c_{gi}^{(m,l,n)}$ corresponds to the weight $-(2n-1)-1+(m-1) = m-2n-1$ terms in the small $\overline{N}$ expansion for $\mathcal{F}_{g/i}^{s(n)}$. For NNLL resummation, only $m = 1, 2, 3$ are needed.

In order to determine the constants relevant for NNLL resummation in (4.18) for all l and n, it turns out that only finite number of input is needed. Let us analyse eq. (4.19) in more detail, taking $\mathcal{F}_{g/i}^{s(n)}(\overline{N},\epsilon)$ as an example. To LL accuracy, one need to determine n unkown coefficients $c_{gi}^{(1,l,n)}$ with $l = 0, \cdots n-1$. The lowest order of ϵ appearing in the ansatz $\mathcal{F}_{g/i}^{s(n)}(\overline{N},\epsilon)$ is ϵ^{-2n+1}. Therefore expanding ϵ to order

$$(-2n+1)+(n-1) = -n \tag{4.21}$$

gives us n conditions and is enough to determine the n unknowns at LL accuracy. To acheive NNLL accuracy, one only needs two more power of ϵ expansion, that is we need to know $\mathcal{F}_{g/i}^{s(n)}(\overline{N},\epsilon)$ to order ϵ^{-n+2}. Similar analysis shows that we also need to know $\mathcal{F}_{q/i}^{s(n)}(\overline{N},\epsilon)$ to order ϵ^{-n+2} to achive NNLL accuracy.

Having this important information in hand, let us contrentrate on the right hand side of eq. (4.15), which generates the necessary ϵ poles. The dimensionally regularized partonic FFs $\widehat{d}^{s}(\overline{N},\epsilon)$ in $\overline{\text{MS}}$ scheme is purely divergent in ϵ and can be determined easily by solving eq. (4.17) order by order in α_s,

$$d\ln\widehat{d}^{s}(\overline{N},\epsilon) = da_s\frac{-\widehat{\gamma}^{T}(\overline{N})}{a_s(\epsilon+\sum_{n=0}^{\infty}{a_s}^{n+1}\beta_n)}\,. \tag{4.22}$$

where we have traded $d\ln\mu^2$ for da_s with the help of the $(4-2\epsilon)$-dimension beta function,

$$\frac{da_s}{d\ln\mu^2} = -2\epsilon a_s - 2a_s \sum_{n=0}^{\infty} {a_s}^{n+1}\beta_n\,. \tag{4.23}$$

Assuming $\widehat{d}^s(\overline{N},\epsilon) = 1 + \sum_{k=1}^{\infty} a_s^k\,\widehat{d}_k^s$ and $\widehat{\gamma}^T(\overline{N}) = \sum_{k=0}^{\infty} {a_s}^{k+1}\widehat{\gamma}_k^T$, the solutions can be worked out order by order. For example, at first four orders we have

$$\begin{aligned}
\widehat{d}_1^s &= -\frac{\widehat{\gamma}_0^T}{\epsilon}\,, \quad \widehat{d}_2^s = \frac{-\widehat{d}_1^s\cdot\widehat{\gamma}_0^T - \widehat{\gamma}_1^T}{2\epsilon} + \frac{\beta_0\widehat{\gamma}_0^T}{2\epsilon^2}\,,\\
\widehat{d}_3^s &= \frac{\beta_0\widehat{d}_1^s\cdot\widehat{\gamma}_0^T + \beta_0\widehat{\gamma}_1^T + \beta_1\widehat{\gamma}_0^T}{3\epsilon^2} + \frac{-\widehat{d}_1^s\cdot\widehat{\gamma}_1^T - \widehat{d}_2^s\cdot\widehat{\gamma}_0^T - \widehat{\gamma}_2^T}{3\epsilon} - \frac{\beta_0^2\widehat{\gamma}_0^T}{3\epsilon^3}\,,\\
\widehat{d}_4^s &= -\frac{\beta_0\left(\beta_0\widehat{d}_1^s.\widehat{\gamma}_0^T + \beta_0\widehat{\gamma}_1^T + 2\beta_1\widehat{\gamma}_0^T\right)}{4\epsilon^3}\\
&\quad + \frac{\beta_0\widehat{d}_1^s.\widehat{\gamma}_1^T + \beta_0\widehat{d}_2^s.\widehat{\gamma}_0^T + \beta_1\widehat{d}_1^s.\widehat{\gamma}_0^T + \beta_0\widehat{\gamma}_2^T + \beta_2\widehat{\gamma}_0^T + \beta_1\widehat{\gamma}_1^T}{4\epsilon^2}\\
&\quad + \frac{-\widehat{d}_1^s.\widehat{\gamma}_2^T - \widehat{d}_2^s.\widehat{\gamma}_1^T - \widehat{d}_3^s.\widehat{\gamma}_0^T - \widehat{\gamma}_3^T}{4\epsilon} + \frac{\beta_0^3\widehat{\gamma}_0^T}{4\epsilon^4}\,.
\end{aligned} \tag{4.24}$$

As explained above, to NNLL accuracy, we need to determine the coefficients of the pole terms in $\mathcal{F}^{s(n)}_{g(q)/i}$ to order ϵ^{-n+2}. Since the matching coefficients $\widehat{C}^s_{g(q)i}(\overline{N},\epsilon)$ in (4.15) must be finite in the limit of $\epsilon\to 0$, we need to determine the coefficients of the pole terms in $\widehat{d}_n^s$ also to order ϵ^{-n+2}. Also recall that $\widehat{d}_n^s$ are function of $\overline{N}$ and we are only interested in the small $\overline{N}$ limit. For NNLL resummation we only need to keep the terms in $\widehat{d}_n^s$ with "small-z" weight up to $2-2n$, see eq. (4.20). We also note that the lowest weight term in $\widehat{\gamma}_n^T$ is $1-2n$, corresponding to the leading $1/\overline{N}^{2n-1}$ pole. Using these information it can be shown that the required inputs for $\widehat{d}_n^s$ to achieve NNLL accuracy are β_0 and $\widehat{\gamma}^T_{0,1,2}$. One can check that this is indeed the case frm eq. (4.24), where explicit examples for $n\le 4$ are shown.

Having known the general form of counter terms $d(\overline{N},\epsilon)$ to any order in α_s, and the fact that the coefficient function $\widehat{C}^s_{g(q)i}$ is finite in the $\epsilon\to 0$ limit, we can solve eq. (4.15) recursively to get the coefficient for the required pole terms in $\mathcal{F}^s_{g(q)/i}$, order by order in α_s. In summary the input data we need to achive NNLL accuracy are

$$\begin{aligned}
&\beta_0\,,\\
&\gamma_0^T\,, \gamma_1^T\,, \gamma_2^T\,,\\
&\mathcal{F}^{s(0)}_{g(q)/i} = 1\,, \mathcal{F}^{s(1)}_{g(q)/i} \text{ to } \epsilon^1\,, \mathcal{F}^{s(2)}_{g(q)/i} \text{ to } \epsilon^0\,.
\end{aligned} \tag{4.25}$$

Note that although we have the explicit results for $\mathcal{F}^{s(3)}_{g(q)/i}$ from direct calculation, they are not needed for predicting the small-z logarithms at NNLL accuracy. Rather they can be used as a check for our resummation.

Following the approach outlined above, we have determined the coefficients of ϵ poles in $\mathcal{F}^{s(n)}_{g(q)/i}$ up to ϵ^{-n+2} for $n\le 15$. From these coefficients we solve for the LL to NNLL constants defined in (4.18). Expanding the results in ϵ gives us the resummed NNLL series truncated at order α_s^{15}, which should be sufficient for phenomenology. We have checked

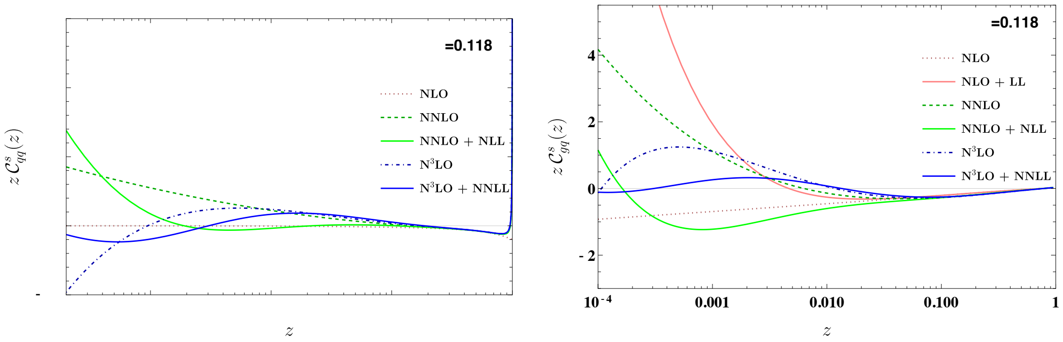

Figure 1. Coefficient functions for quark TMD FFs. Shown in the plots are fixed-order results at NLO, NNLO and N^{3}LO, as well as adding the higher-order resummation contributions truncated to order α_s^{15}.

that a truncation of perturbative series at α_s^{15} leads to a less that 1% relative uncertainty. The analytic expressions for the truncated resummed perturbative series can be found in the supplementary material attached to this paper.

At LL, we are able to find the generating function for the series

$$\widehat{C}^s_{gq}(\overline{N})|_{\rm LL} = \sum_{n=1}^{\infty} a_s^n \overline{N}^{-2n} C_F C_A^{n-1} A_n \,, \tag{4.26}$$

with

$$A_n = \frac{(-1)^n 2^{5n} \Gamma\left(n + \frac{1}{4}\right)}{\Gamma\left(\frac{1}{4}\right) \Gamma(n+1)} \,.$$

The series can be resummed analytically, leading to an closed form expression for LL results,

$$\widehat{C}^s_{gg}(\overline{N})|_{\rm LL} = \frac{C_A}{C_F} \widehat{C}^s_{gq}(\overline{N})|_{\rm LL} = \left(1 + \frac{32 C_A a_s}{\overline{N}^2}\right)^{-1/4} - 1 \,. \tag{4.27}$$

It's interesting to note that eq. (4.27) coincides with that of the transverse coefficient functions for semi-inclusive e^+e^- annihilation [56, 79].

In figure 1 and 2 we plot the fixed-order coefficient functions and with different orders of small-z resummation. We use $N_f = 5$ throughout the calculations. We note that even at N^{3}LO, the effects of resummation is important for $z < 10^{-2}$.

5 Conclusion

In summary we presented calculations for the unpolarized quark and gluon TMD PDFs and FFs at N^{3}LO in QCD. The unpolarized quark TMD PDFs at N^{3}LO have already been reported in ref. [47]. The rest of the calculations are new. Unpolarized quark and gluon TMD PDFs have also been calculated in [48] recently using an independent method, whose results are in full agreement with ours.[2]

[2]Except for a minor error in an anomalous color factor in [47], which has been corrected in the arXiv version of that paper.

JHEP06(2021)115

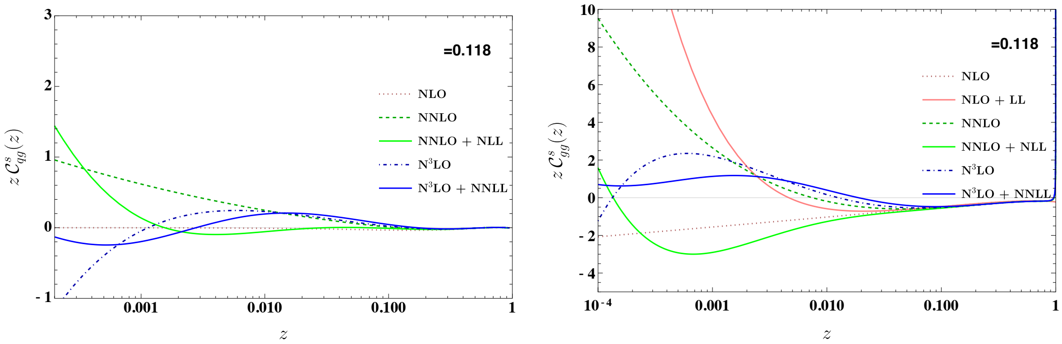

Figure 2. Coefficient functions for gluon TMD FFs. Shown in the plots are fixed-order results at NLO, NNLO and N^{3}LO, as well as adding the higher-order resummation contributions truncated to order α_s^{15}.

Our calculations for TMD PDFs are based on the method proposed in [47], which in turns is based on decomposition of light-cone correlators into phase space integration of collinear splitting amplitudes of different multiplicities. The advantage of this decomposition is that it allows better understanding of the analytic continuation property of TMD PDFs and FFs [50]. Using the analytic continuation prescription of [50], we successfully obtained the N^{3}LO TMD FFs from corresponding TMD PDFs, without the need to compute everything from scratch. Our results open the avenue for precision phenomenology of TMD physics at N^{3}LO in perturbative QCD.

We also provide threshold and high energy asymptotics of TMD PDFs and FFs through N^{3}LO by expanding the corresponding analytic expressions. The high energy (small-z) limit of TMD FFs features double logarithmic enhancement, in contrast to the single logarithmic enhancement of TMD PDFs. We resum the small-z logarithms through NNLL accuracy using a method proposed in [56]. The resummation leads to better behaved perturbative convergence for $z < 10^{-2}$.

Our method of calculation is general and is not limited to unpolarized distribution. Works towards to polarized TMD distributions at N^{3}LO are in progress.

Note added. A few days after this paper appeared, an independent calculation for unpolarized quark and gluon TMD FFs at N^{3}LO was submitted to arXiv [80]. During private communication, the Authors of [80] uncovered a minor error in one of their routine for analytic continuation. After fixing it, they found full agreement with our results.

Acknowledgments

We thank Duff Neill and Simone Marzani for useful discussion. We also thank Markus Ebert, Bernhard Mistlberger, Gherardo Vita for useful correspondence. This work was supported in part by the National Science Foundation of China under contract No. 11975200 and No. 11935013. T.Z.Y. also want to acknowledge the support from the Swiss National Science Foundation (SNF) under contract 200020-175595.

A QCD beta function

The QCD beta function is defined as

$$\frac{d\alpha_s}{d\ln\mu} = \beta(\alpha_s) = -2\alpha_s \sum_{n=0}^{\infty} \left(\frac{\alpha_s}{4\pi}\right)^{n+1} \beta_n\,, \tag{A.1}$$

with [81]

$$\begin{aligned}
\beta_0 &= \frac{11}{3}C_A - \frac{4}{3}T_F N_f\,,\\
\beta_1 &= \frac{34}{3}C_A^2 - \frac{20}{3}C_A T_F N_f - 4C_F T_F N_f\,,\\
\beta_2 &= \left(\frac{158C_A}{27} + \frac{44C_F}{9}\right) N_f^2 T_F^2 + \left(-\frac{205C_A C_F}{9} - \frac{1415C_A^2}{27} + 2C_F^2\right) N_f T_F + \frac{2857C_A^3}{54}\,.
\end{aligned} \tag{A.2}$$

B Anomalous dimension

For all the anomalous dimensions entering the renormalization group equations of various TMD functions, we define the perturbative expansion in α_s according to

$$\gamma(\alpha_s) = \sum_{n=0}^{\infty} \left(\frac{\alpha_s}{4\pi}\right)^{n+1} \gamma_n\,, \tag{B.1}$$

where the coefficients for quark are given by

$$\begin{aligned}
\Gamma_0^{\rm cusp} &= 4C_F\,,\\
\Gamma_1^{\rm cusp} &= \left(\frac{268}{9} - 8\zeta_2\right) C_A C_F - \frac{80C_F T_F N_f}{9}\,,\\
\Gamma_2^{\rm cusp} &= \left[\left(\frac{320\zeta_2}{9} - \frac{224\zeta_3}{3} - \frac{1672}{27}\right) C_A C_F + \left(64\zeta_3 - \frac{220}{3}\right) C_F^2\right] N_f T_F\\
&\quad + \left(-\frac{1072\zeta_2}{9} + \frac{88\zeta_3}{3} + 88\zeta_4 + \frac{490}{3}\right) C_A^2 C_F - \frac{64}{27} C_F N_f^2 T_F^2\,,\\
\gamma_0^S &= 0\,,\\
\gamma_1^S &= \left[\left(-\frac{404}{27} + \frac{11\zeta_2}{3} + 14\zeta_3\right) C_A + \left(\frac{112}{27} - \frac{4\zeta_2}{3}\right) T_F N_f\right] C_F\,,\\
\gamma_2^S &= \left(-\frac{88}{3}\zeta_3\zeta_2 + \frac{6325\zeta_2}{81} + \frac{658\zeta_3}{3} - 88\zeta_4 - 96\zeta_5 - \frac{136781}{1458}\right) C_A^2 C_F + \left(\frac{80\zeta_2}{27} - \frac{224\zeta_3}{27}\right.\\
&\quad \left. + \frac{4160}{729}\right) C_F N_f^2 T_F^2 + \left(-\frac{2828\zeta_2}{81} - \frac{728\zeta_3}{27} + 48\zeta_4 + \frac{11842}{729}\right) C_A C_F N_f T_F\\
&\quad + \left(-4\zeta_2 - \frac{304\zeta_3}{9} - 16\zeta_4 + \frac{1711}{27}\right) C_F^2 N_f T_F\,.\\
\gamma_0^R &= 0\,,\\
\gamma_1^R &= \left[\left(-\frac{404}{27} + 14\zeta_3\right) C_A + \frac{112}{27} T_F N_f\right] C_F\,,
\end{aligned}$$

$$
\begin{aligned}
\gamma_2^R = \Bigg[& \left(-\frac{824\zeta_2}{81}-\frac{904\zeta_3}{27}+\frac{20\zeta_4}{3}+\frac{62626}{729}\right) C_A N_f T_F + \left(-\frac{88}{3}\zeta_3\zeta_2+\frac{3196\zeta_2}{81}+\frac{6164\zeta_3}{27}\right. \\
& \left. +\frac{77\zeta_4}{3}-96\zeta_5-\frac{297029}{1458}\right) C_A^2 + \left(-\frac{304\zeta_3}{9}-16\zeta_4+\frac{1711}{27}\right) C_F N_f T_F + \left(-\frac{64\zeta_3}{9}\right. \\
& \left. -\frac{3712}{729}\right) N_f^2 T_F^2 \Bigg] C_F \,.
\end{aligned} \tag{B.2}
$$

Since cusp and soft and rapidity anomalous dimensions exhibit Casimir scaling, the corresponding anomalous dimensions for gluon could be obtained by multiplying in above with C_A/C_F.

The beam anomalous dimensions do not exhibits Casimir scaling, thus should be list separately. The beam anomalous dimensions for quark are

$$
\begin{aligned}
\gamma_0^B = {} & 3C_F \,, \\
\gamma_1^B = {} & \left[\left(\frac{3}{2}-12\zeta_2+24\zeta_3\right) C_F + \left(\frac{17}{6}+\frac{44\zeta_2}{3}-12\zeta_3\right) C_A + \left(-\frac{2}{3}-\frac{16\zeta_2}{3}\right) T_F N_f\right] C_F, \\
\gamma_2^B = {} & \left[\left(-\frac{2672\zeta_2}{27}+\frac{400\zeta_3}{9}+4\zeta_4+40\right) C_A C_F + \left(\frac{40\zeta_2}{3}-\frac{272\zeta_3}{3}+\frac{232\zeta_4}{3}-46\right) C_F^2\right] N_f T_F \\
& + \left(16\zeta_3\zeta_2-\frac{410\zeta_2}{3}+\frac{844\zeta_3}{3}-\frac{494\zeta_4}{3}+120\zeta_5+\frac{151}{4}\right) C_A C_F^2 + \left(\frac{320\zeta_2}{27}-\frac{64\zeta_3}{9}-\frac{68}{9}\right) \\
& \times C_F N_f^2 T_F^2 + \left(\frac{4496\zeta_2}{27}-\frac{1552\zeta_3}{9}-5\zeta_4+40\zeta_5-\frac{1657}{36}\right) C_A^2 C_F + \left(-32\zeta_3\zeta_2+18\zeta_2\right. \\
& \left. +68\zeta_3+144\zeta_4-240\zeta_5+\frac{29}{2}\right) C_F^3 \,.
\end{aligned} \tag{B.3}
$$

The beam anomalous dimensions for gluon are

$$
\begin{aligned}
\gamma_0^B = {} & \frac{11}{3} C_A - \frac{4}{3} T_F N_f \,, \\
\gamma_1^B = {} & C_A^2 \left(\frac{32}{3}+12\zeta_3\right) + \left(-\frac{16}{3} C_A - 4C_F\right) N_f T_F \,, \\
\gamma_2^B = {} & C_A^3 \left(-80\zeta_5-16\zeta_3\zeta_2+\frac{55}{3}\zeta_4+\frac{536}{3}\zeta_3+\frac{8}{3}\zeta_2+\frac{79}{2}\right) \\
& + C_A^2 N_f T_F \left(-\frac{20}{3}\zeta_4-\frac{160}{3}\zeta_3-\frac{16}{3}\zeta_2-\frac{233}{9}\right) + \frac{58}{9} C_A N_f^2 T_F^2 - \frac{241}{9} C_A C_F N_f T_F \\
& + 2C_F^2 N_f T_F + \frac{44}{9} C_F N_f^2 T_F^2 \,.
\end{aligned} \tag{B.4}
$$

The cusp anomalous dimension Γ^{cusp} can be found in [65]. The beam anomalous dimension γ^B is related to the soft anomalous dimension γ^S [82] and the hard anomalous dimensions γ^H [83–85] by renormalization group invariance condition $\gamma^B = \gamma^S - \gamma^H$. The rapidity anomalous dimension γ^R can be found in [69, 73]. Note that the normalization here differ from those in [69] by a factor of 1/2.

C Renormalization constants

The following constants are needed for the renormalization of zero-bin subtracted [64] TMD PDFs through N^{3}LO, see e.g. refs. [26, 27]. The first three-order corrections to Z^B and

Z^S are

$$
\begin{aligned}
Z_1^B &= \frac{1}{2\epsilon}\left(2\gamma_0^B - \Gamma_0^{\rm cusp} L_Q\right), \\
Z_2^B &= \frac{1}{8\epsilon^2}\left((\Gamma_0^{\rm cusp} L_Q - 2\gamma_0^B)^2 + 2\beta_0(\Gamma_0^{\rm cusp} L_Q - 2\gamma_0^B)\right) + \frac{1}{4\epsilon}\left(2\gamma_1^B - \Gamma_1^{\rm cusp} L_Q\right), \\
Z_3^B &= \frac{1}{48\epsilon^3}\left(2\gamma_0^B - \Gamma_0^{\rm cusp} L_Q\right)\left(8\beta_0^2 + 6\beta_0\left(-2\gamma_0^B + \Gamma_0^{\rm cusp} L_Q\right) + \left(-2\gamma_0^B + \Gamma_0^{\rm cusp} L_Q\right)^2\right) \\
&\quad + \frac{1}{24\epsilon^2}\left(\beta_1\left(-8\gamma_0^B + 4\Gamma_0^{\rm cusp} L_Q\right) + \left(4\beta_0 - 6\gamma_0^B + 3\Gamma_0^{\rm cusp} L_Q\right)\left(-2\gamma_1^B + \Gamma_1^{\rm cusp} L_Q\right)\right) \\
&\quad + \frac{1}{6\epsilon}\left(2\gamma_2^B - \Gamma_2^{\rm cusp} L_Q\right) \\
Z_1^S &= \frac{1}{\epsilon^2}\Gamma_0^{\rm cusp} + \frac{1}{\epsilon}\left(-2\gamma_0^S - \Gamma_0^{\rm cusp} L_\nu\right), \\
Z_2^S &= \frac{1}{2\epsilon^4}(\Gamma_0^{\rm cusp})^2 - \frac{1}{4\epsilon^3}\left(\Gamma_0^{\rm cusp}(3\beta_0 + 8\gamma_0^S) + 4(\Gamma_0^{\rm cusp})^2 L_\nu\right) - \frac{1}{2\epsilon}\left(2\gamma_1^S + \Gamma_1^{\rm cusp} L_\nu\right) \\
&\quad + \frac{1}{4\epsilon^2}\left(\Gamma_1^{\rm cusp} + 2(2\gamma_0^S + \Gamma_0^{\rm cusp} L_\nu)(\beta_0 + 2\gamma_0^S + \Gamma_0^{\rm cusp} L_\nu)\right), \\
Z_3^S &= \frac{1}{6\epsilon^6}(\Gamma_0^{\rm cusp})^3 - \frac{1}{4\epsilon^5}(\Gamma_0^{\rm cusp})^2\left(3\beta_0 + 4\gamma_0^S + 2\Gamma_0^{\rm cusp} L_\nu\right) + \frac{1}{36\epsilon^4}\Gamma_0^{\rm cusp}\left(22\beta_0^2 + 45\beta_0\left(2\gamma_0^S + \Gamma_0^{\rm cusp} L_\nu\right)\right. \\
&\quad \left. + 9\left(\Gamma_1^{\rm cusp} + 2\left(2\gamma_0^S + \Gamma_0^{\rm cusp} L_\nu\right)^2\right)\right) + \frac{1}{36\epsilon^3}\left(-16\beta_1\Gamma_0^{\rm cusp} - 12\beta_0^2\left(2\gamma_0^S + \Gamma_0^{\rm cusp} L_\nu\right)\right. \\
&\quad - 2\beta_0\left(5\Gamma_1^{\rm cusp} + 9\left(2\gamma_0^S + \Gamma_0^{\rm cusp} L_\nu\right)^2\right) - 3\left[\Gamma_1^{\rm cusp}\left(6\gamma_0^S + 9\Gamma_0^{\rm cusp} L_\nu\right)\right. \\
&\quad \left.\left. + 2\left(8\left(\gamma_0^S\right)^3 + 6\Gamma_0^{\rm cusp}\gamma_1^S + 12\Gamma_0^{\rm cusp}\left(\gamma_0^S\right)^2 L_\nu + 6(\Gamma_0^{\rm cusp})^2\gamma_0^S L_\nu^2 + (\Gamma_0^{\rm cusp})^3 L_\nu^3\right)\right]\right) \\
&\quad + \frac{1}{18\epsilon^2}\left(2\Gamma_2^{\rm cusp} + 3\left(2\beta_1\left(2\gamma_0^S + \Gamma_0^{\rm cusp} L_\nu\right) + \left(2\beta_0 + 6\gamma_0^S + 3\Gamma_0^{\rm cusp} L_\nu\right)\left(2\gamma_1^S + \Gamma_1^{\rm cusp} L_\nu\right)\right)\right) \\
&\quad - \frac{2\gamma_2^S + \Gamma_2^{\rm cusp} L_\nu}{3\epsilon}.
\end{aligned} \tag{C.1}
$$

Keep in mind that the anomalous dimensions appeared above depends on the flavor, they should be replaced by the corresponding values in section B. We also remind the reader that the renormalization constants are formally identical for TMD PDFs and TMD FFs, the logarithms appeared above should be replaced by their corresponding values in each case, and we have

$$
L_\perp = \ln\frac{b_T^2\mu^2}{b_0^2}, \quad L_\nu = \ln\frac{\nu^2}{\mu^2}, \tag{C.2}
$$

with $b_0 = 2\,e^{-\gamma_E}$ for both TMD PDFs and TMD FFs.

For TMD PDFs,

$$
L_Q = 2\ln\frac{x\,P_+}{\nu}, \tag{C.3}
$$

while for TMD FFs,

$$
L_Q = 2\ln\frac{P_+}{z\,\nu}. \tag{C.4}
$$

References

[1] D. Boer et al., *Gluons and the quark sea at high energies: Distributions, polarization, tomography*, arXiv:1108.1713 [INSPIRE].

[2] A. Accardi et al., *Electron Ion Collider: The Next QCD Frontier*: Understanding the glue that binds us all, *Eur. Phys. J. A* **52** (2016) 268 [arXiv:1212.1701] [INSPIRE].

[3] R. Angeles-Martinez et al., *Transverse Momentum Dependent (TMD) parton distribution functions: status and prospects*, *Acta Phys. Polon. B* **46** (2015) 2501 [arXiv:1507.05267] [INSPIRE].

[4] Y.L. Dokshitzer, D. Diakonov and S.I. Troian, *On the Transverse Momentum Distribution of Massive Lepton Pairs*, *Phys. Lett. B* **79** (1978) 269 [INSPIRE].

[5] G. Parisi and R. Petronzio, *Small Transverse Momentum Distributions in Hard Processes*, *Nucl. Phys. B* **154** (1979) 427 [INSPIRE].

[6] J.C. Collins and D.E. Soper, *Parton Distribution and Decay Functions*, *Nucl. Phys. B* **194** (1982) 445 [INSPIRE].

[7] J.C. Collins, D.E. Soper and G.F. Sterman, *Transverse Momentum Distribution in Drell-Yan Pair and W and Z Boson Production*, *Nucl. Phys. B* **250** (1985) 199 [INSPIRE].

[8] X.-d. Ji, J.-P. Ma and F. Yuan, *QCD factorization for spin-dependent cross sections in DIS and Drell-Yan processes at low transverse momentum*, *Phys. Lett. B* **597** (2004) 299 [hep-ph/0405085] [INSPIRE].

[9] X.-d. Ji, J.-p. Ma and F. Yuan, *QCD factorization for semi-inclusive deep-inelastic scattering at low transverse momentum*, *Phys. Rev. D* **71** (2005) 034005 [hep-ph/0404183] [INSPIRE].

[10] G. Bozzi, S. Catani, D. de Florian and M. Grazzini, *Transverse-momentum resummation and the spectrum of the Higgs boson at the LHC*, *Nucl. Phys. B* **737** (2006) 73 [hep-ph/0508068] [INSPIRE].

[11] I.O. Cherednikov and N.G. Stefanis, *Renormalization, Wilson lines, and transverse-momentum dependent parton distribution functions*, *Phys. Rev. D* **77** (2008) 094001 [arXiv:0710.1955] [INSPIRE].

[12] J. Collins, *Foundations of perturbative QCD*, *Camb. Monogr. Part. Phys. Nucl. Phys. Cosmol.* **32** (2011) 1 [INSPIRE].

[13] T. Becher and M. Neubert, *Drell-Yan Production at Small q_T, Transverse Parton Distributions and the Collinear Anomaly*, *Eur. Phys. J. C* **71** (2011) 1665 [arXiv:1007.4005] [INSPIRE].

[14] M.G. Echevarria, A. Idilbi, A. Schäfer and I. Scimemi, *Model-Independent Evolution of Transverse Momentum Dependent Distribution Functions (TMDs) at NNLL*, *Eur. Phys. J. C* **73** (2013) 2636 [arXiv:1208.1281] [INSPIRE].

[15] J.-Y. Chiu, A. Jain, D. Neill and I.Z. Rothstein, *A Formalism for the Systematic Treatment of Rapidity Logarithms in Quantum Field Theory*, *JHEP* **05** (2012) 084 [arXiv:1202.0814] [INSPIRE].

JHEP06(2021)115

[16] S. Catani and M. Grazzini, *Higgs Boson Production at Hadron Colliders: Hard-Collinear Coefficients at the NNLO*, Eur. Phys. J. C **72** (2012) 2013 [*Erratum ibid.* **72** (2012) 2132] [arXiv:1106.4652] [INSPIRE].

[17] S. Catani, L. Cieri, D. de Florian, G. Ferrera and M. Grazzini, *Vector boson production at hadron colliders: hard-collinear coefficients at the NNLO*, Eur. Phys. J. C **72** (2012) 2195 [arXiv:1209.0158] [INSPIRE].

[18] T. Becher and G. Bell, *Analytic Regularization in Soft-Collinear Effective Theory*, Phys. Lett. B **713** (2012) 41 [arXiv:1112.3907] [INSPIRE].

[19] J.-y. Chiu, A. Fuhrer, A.H. Hoang, R. Kelley and A.V. Manohar, *Soft-Collinear Factorization and Zero-Bin Subtractions*, Phys. Rev. D **79** (2009) 053007 [arXiv:0901.1332] [INSPIRE].

[20] M.G. Echevarria, I. Scimemi and A. Vladimirov, *Universal transverse momentum dependent soft function at NNLO*, Phys. Rev. D **93** (2016) 054004 [arXiv:1511.05590] [INSPIRE].

[21] Y. Li, D. Neill and H.X. Zhu, *An exponential regulator for rapidity divergences*, Nucl. Phys. B **960** (2020) 115193 [arXiv:1604.00392] [INSPIRE].

[22] M.A. Ebert, I. Moult, I.W. Stewart, F.J. Tackmann, G. Vita and H.X. Zhu, *Subleading power rapidity divergences and power corrections for q_T*, JHEP **04** (2019) 123 [arXiv:1812.08189] [INSPIRE].

[23] T. Gehrmann, T. Lubbert and L.L. Yang, *Transverse parton distribution functions at next-to-next-to-leading order: the quark-to-quark case*, Phys. Rev. Lett. **109** (2012) 242003 [arXiv:1209.0682] [INSPIRE].

[24] T. Gehrmann, T. Luebbert and L.L. Yang, *Calculation of the transverse parton distribution functions at next-to-next-to-leading order*, JHEP **06** (2014) 155 [arXiv:1403.6451] [INSPIRE].

[25] M.G. Echevarria, I. Scimemi and A. Vladimirov, *Unpolarized Transverse Momentum Dependent Parton Distribution and Fragmentation Functions at next-to-next-to-leading order*, JHEP **09** (2016) 004 [arXiv:1604.07869] [INSPIRE].

[26] M.-X. Luo, X. Wang, X. Xu, L.L. Yang, T.-Z. Yang and H.X. Zhu, *Transverse Parton Distribution and Fragmentation Functions at NNLO: the Quark Case*, JHEP **10** (2019) 083 [arXiv:1908.03831] [INSPIRE].

[27] M.-X. Luo, T.-Z. Yang, H.X. Zhu and Y.J. Zhu, *Transverse Parton Distribution and Fragmentation Functions at NNLO: the Gluon Case*, JHEP **01** (2020) 040 [arXiv:1909.13820] [INSPIRE].

[28] D. Gutierrez-Reyes, S. Leal-Gomez, I. Scimemi and A. Vladimirov, *Linearly polarized gluons at next-to-next-to leading order and the Higgs transverse momentum distribution*, JHEP **11** (2019) 121 [arXiv:1907.03780] [INSPIRE].

[29] S. Catani and M. Grazzini, *An NNLO subtraction formalism in hadron collisions and its application to Higgs boson production at the LHC*, Phys. Rev. Lett. **98** (2007) 222002 [hep-ph/0703012] [INSPIRE].

[30] S. Catani, L. Cieri, G. Ferrera, D. de Florian and M. Grazzini, *Vector boson production at hadron colliders: a fully exclusive QCD calculation at NNLO*, Phys. Rev. Lett. **103** (2009) 082001 [arXiv:0903.2120] [INSPIRE].

[31] G. Bozzi, S. Catani, D. de Florian and M. Grazzini, *The q_T spectrum of the Higgs boson at the LHC in QCD perturbation theory*, Phys. Lett. B **564** (2003) 65 [hep-ph/0302104] [INSPIRE].

JHEP06(2021)115

[32] L.-B. Chen, H.T. Li, H.-S. Shao and J. Wang, *Higgs boson pair production via gluon fusion at N^{3}LO in QCD*, *Phys. Lett. B* **803** (2020) 135292 [arXiv:1909.06808] [INSPIRE].

[33] L.-B. Chen, H.T. Li, H.-S. Shao and J. Wang, *The gluon-fusion production of Higgs boson pair: N^{3}LO QCD corrections and top-quark mass effects*, *JHEP* **03** (2020) 072 [arXiv:1912.13001] [INSPIRE].

[34] L. Cieri, X. Chen, T. Gehrmann, E.W.N. Glover and A. Huss, *Higgs boson production at the LHC using the q_T subtraction formalism at N^{3}LO QCD*, *JHEP* **02** (2019) 096 [arXiv:1807.11501] [INSPIRE].

[35] X. Chen et al., *Precise QCD Description of the Higgs Boson Transverse Momentum Spectrum*, *Phys. Lett. B* **788** (2019) 425 [arXiv:1805.00736] [INSPIRE].

[36] W. Bizoń et al., *Fiducial distributions in Higgs and Drell-Yan production at N^{3}LL+NNLO*, *JHEP* **12** (2018) 132 [arXiv:1805.05916] [INSPIRE].

[37] W. Bizon et al., *The transverse momentum spectrum of weak gauge bosons at N^{3}LL+NNLO*, *Eur. Phys. J. C* **79** (2019) 868 [arXiv:1905.05171] [INSPIRE].

[38] V. Bertone, I. Scimemi and A. Vladimirov, *Extraction of unpolarized quark transverse momentum dependent parton distributions from Drell-Yan/Z-boson production*, *JHEP* **06** (2019) 028 [arXiv:1902.08474] [INSPIRE].

[39] A. Bacchetta et al., *Transverse-momentum-dependent parton distributions up to N^{3}LL from Drell-Yan data*, *JHEP* **07** (2020) 117 [arXiv:1912.07550] [INSPIRE].

[40] M.A. Ebert, J.K.L. Michel, I.W. Stewart and F.J. Tackmann, *Drell-Yan q_T resummation of fiducial power corrections at N^{3}LL*, *JHEP* **04** (2021) 102 [arXiv:2006.11382] [INSPIRE].

[41] T. Becher and T. Neumann, *Fiducial q_T resummation of color-singlet processes at N^{3}LL+NNLO*, *JHEP* **03** (2021) 199 [arXiv:2009.11437] [INSPIRE].

[42] M.A. Ebert, I.W. Stewart and Y. Zhao, *Towards Quasi-Transverse Momentum Dependent PDFs Computable on the Lattice*, *JHEP* **09** (2019) 037 [arXiv:1901.03685] [INSPIRE].

[43] X. Ji, Y. Liu and Y.-S. Liu, *Transverse-momentum-dependent parton distribution functions from large-momentum effective theory*, *Phys. Lett. B* **811** (2020) 135946 [arXiv:1911.03840] [INSPIRE].

[44] M.A. Ebert, I.W. Stewart and Y. Zhao, *Renormalization and Matching for the Collins-Soper Kernel from Lattice QCD*, *JHEP* **03** (2020) 099 [arXiv:1910.08569] [INSPIRE].

[45] Lattice Parton collaboration, *Lattice QCD Calculations of Transverse-Momentum-Dependent Soft Function through Large-Momentum Effective Theory*, *Phys. Rev. Lett.* **125** (2020) 192001 [arXiv:2005.14572] [INSPIRE].

[46] M.A. Ebert, S.T. Schindler, I.W. Stewart and Y. Zhao, *One-loop Matching for Spin-Dependent Quasi-TMDs*, *JHEP* **09** (2020) 099 [arXiv:2004.14831] [INSPIRE].

[47] M.-x. Luo, T.-Z. Yang, H.X. Zhu and Y.J. Zhu, *Quark Transverse Parton Distribution at the Next-to-Next-to-Next-to-Leading Order*, *Phys. Rev. Lett.* **124** (2020) 092001 [arXiv:1912.05778] [INSPIRE].

[48] M.A. Ebert, B. Mistlberger and G. Vita, *Transverse momentum dependent PDFs at N^{3}LO*, *JHEP* **09** (2020) 146 [arXiv:2006.05329] [INSPIRE].

[49] M.A. Ebert, B. Mistlberger and G. Vita, *Collinear expansion for color singlet cross sections*, *JHEP* **09** (2020) 181 [arXiv:2006.03055] [INSPIRE].

JHEP06(2021)115

[50] H. Chen, T.-Z. Yang, H.X. Zhu and Y.J. Zhu, *Analytic Continuation and Reciprocity Relation for Collinear Splitting in QCD*, *Chin. Phys. C* **45** (2021) 043101 [arXiv:2006.10534] [INSPIRE].

[51] A. Mitov, S. Moch and A. Vogt, *Next-to-Next-to-Leading Order Evolution of Non-Singlet Fragmentation Functions*, *Phys. Lett. B* **638** (2006) 61 [hep-ph/0604053] [INSPIRE].

[52] S. Moch and A. Vogt, *On third-order timelike splitting functions and top-mediated Higgs decay into hadrons*, *Phys. Lett. B* **659** (2008) 290 [arXiv:0709.3899] [INSPIRE].

[53] A.A. Almasy, S. Moch and A. Vogt, *On the Next-to-Next-to-Leading Order Evolution of Flavour-Singlet Fragmentation Functions*, *Nucl. Phys. B* **854** (2012) 133 [arXiv:1107.2263] [INSPIRE].

[54] E. Remiddi and J.A.M. Vermaseren, *Harmonic polylogarithms*, *Int. J. Mod. Phys. A* **15** (2000) 725 [hep-ph/9905237] [INSPIRE].

[55] D. Neill and F. Ringer, *Soft Fragmentation on the Celestial Sphere*, *JHEP* **06** (2020) 086 [arXiv:2003.02275] [INSPIRE].

[56] A. Vogt, *Resummation of small-x double logarithms in QCD: semi-inclusive electron-positron annihilation*, *JHEP* **10** (2011) 025 [arXiv:1108.2993] [INSPIRE].

[57] C.H. Kom, A. Vogt and K. Yeats, *Resummed small-x and first-moment evolution of fragmentation functions in perturbative QCD*, *JHEP* **10** (2012) 033 [arXiv:1207.5631] [INSPIRE].

[58] C.W. Bauer, S. Fleming and M.E. Luke, *Summing Sudakov logarithms in $B \to X_s\gamma$ in effective field theory*, *Phys. Rev. D* **63** (2000) 014006 [hep-ph/0005275] [INSPIRE].

[59] C.W. Bauer, S. Fleming, D. Pirjol and I.W. Stewart, *An Effective field theory for collinear and soft gluons: Heavy to light decays*, *Phys. Rev. D* **63** (2001) 114020 [hep-ph/0011336] [INSPIRE].

[60] C.W. Bauer, D. Pirjol and I.W. Stewart, *Soft collinear factorization in effective field theory*, *Phys. Rev. D* **65** (2002) 054022 [hep-ph/0109045] [INSPIRE].

[61] C.W. Bauer, S. Fleming, D. Pirjol, I.Z. Rothstein and I.W. Stewart, *Hard scattering factorization from effective field theory*, *Phys. Rev. D* **66** (2002) 014017 [hep-ph/0202088] [INSPIRE].

[62] M. Beneke, A.P. Chapovsky, M. Diehl and T. Feldmann, *Soft collinear effective theory and heavy to light currents beyond leading power*, *Nucl. Phys. B* **643** (2002) 431 [hep-ph/0206152] [INSPIRE].

[63] C.W. Bauer and I.W. Stewart, *Invariant operators in collinear effective theory*, *Phys. Lett. B* **516** (2001) 134 [hep-ph/0107001] [INSPIRE].

[64] A.V. Manohar and I.W. Stewart, *The Zero-Bin and Mode Factorization in Quantum Field Theory*, *Phys. Rev. D* **76** (2007) 074002 [hep-ph/0605001] [INSPIRE].

[65] S. Moch, J.A.M. Vermaseren and A. Vogt, *The Three loop splitting functions in QCD: The Nonsinglet case*, *Nucl. Phys. B* **688** (2004) 101 [hep-ph/0403192] [INSPIRE].

[66] A. Vogt, S. Moch and J.A.M. Vermaseren, *The Three-loop splitting functions in QCD: The Singlet case*, *Nucl. Phys. B* **691** (2004) 129 [hep-ph/0404111] [INSPIRE].

[67] J. Ablinger, A. Behring, J. Blümlein, A. De Freitas, A. von Manteuffel and C. Schneider, *The 3-loop pure singlet heavy flavor contributions to the structure function $F_2(x, Q^2)$ and the anomalous dimension*, *Nucl. Phys. B* **890** (2014) 48 [arXiv:1409.1135] [INSPIRE].

[68] J. Ablinger, A. Behring, J. Blümlein, A. De Freitas, A. von Manteuffel and C. Schneider, *The three-loop splitting functions $P_{qg}^{(2)}$ and $P_{gg}^{(2,N_F)}$*, *Nucl. Phys. B* **922** (2017) 1 [arXiv:1705.01508] [INSPIRE].

[69] Y. Li and H.X. Zhu, *Bootstrapping Rapidity Anomalous Dimensions for Transverse-Momentum Resummation*, *Phys. Rev. Lett.* **118** (2017) 022004 [arXiv:1604.01404] [INSPIRE].

[70] I. Moult and H.X. Zhu, *Simplicity from Recoil: The Three-Loop Soft Function and Factorization for the Energy-Energy Correlation*, *JHEP* **08** (2018) 160 [arXiv:1801.02627] [INSPIRE].

[71] Y.J. Zhu, *Double soft current at one-loop in QCD*, arXiv:2009.08919 [INSPIRE].

[72] J.-y. Chiu, A. Jain, D. Neill and I.Z. Rothstein, *The Rapidity Renormalization Group*, *Phys. Rev. Lett.* **108** (2012) 151601 [arXiv:1104.0881] [INSPIRE].

[73] A.A. Vladimirov, *Correspondence between Soft and Rapidity Anomalous Dimensions*, *Phys. Rev. Lett.* **118** (2017) 062001 [arXiv:1610.05791] [INSPIRE].

[74] G. Lustermans, W.J. Waalewijn and L. Zeune, *Joint transverse momentum and threshold resummation beyond NLL*, *Phys. Lett. B* **762** (2016) 447 [arXiv:1605.02740] [INSPIRE].

[75] G. Billis, M.A. Ebert, J.K.L. Michel and F.J. Tackmann, *A toolbox for q_T and 0-jettiness subtractions at N^3LO*, *Eur. Phys. J. Plus* **136** (2021) 214 [arXiv:1909.00811] [INSPIRE].

[76] S. Moch, B. Ruijl, T. Ueda, J.A.M. Vermaseren and A. Vogt, *Four-Loop Non-Singlet Splitting Functions in the Planar Limit and Beyond*, *JHEP* **10** (2017) 041 [arXiv:1707.08315] [INSPIRE].

[77] D. Maître, *HPL, a mathematica implementation of the harmonic polylogarithms*, *Comput. Phys. Commun.* **174** (2006) 222 [hep-ph/0507152] [INSPIRE].

[78] S. Marzani, *Combining Q_T and small-x resummations*, *Phys. Rev. D* **93** (2016) 054047 [arXiv:1511.06039] [INSPIRE].

[79] S. Albino, P. Bolzoni, B.A. Kniehl and A. Kotikov, *Fully double-logarithm-resummed cross sections*, *Nucl. Phys. B* **851** (2011) 86 [arXiv:1104.3018] [INSPIRE].

[80] M.A. Ebert, B. Mistlberger and G. Vita, *TMD Fragmentation Functions at N^3LO*, arXiv:2012.07853 [INSPIRE].

[81] P.A. Baikov, K.G. Chetyrkin and J.H. Kühn, *Five-Loop Running of the QCD coupling constant*, *Phys. Rev. Lett.* **118** (2017) 082002 [arXiv:1606.08659] [INSPIRE].

[82] Y. Li, A. von Manteuffel, R.M. Schabinger and H.X. Zhu, *Soft-virtual corrections to Higgs production at N^3LO*, *Phys. Rev. D* **91** (2015) 036008 [arXiv:1412.2771] [INSPIRE].

[83] S. Moch, J.A.M. Vermaseren and A. Vogt, *Three-loop results for quark and gluon form-factors*, *Phys. Lett. B* **625** (2005) 245 [hep-ph/0508055] [INSPIRE].

[84] T. Gehrmann, E.W.N. Glover, T. Huber, N. Ikizlerli and C. Studerus, *Calculation of the quark and gluon form factors to three loops in QCD*, *JHEP* **06** (2010) 094 [arXiv:1004.3653] [INSPIRE].

[85] T. Becher and M. Neubert, *On the Structure of Infrared Singularities of Gauge-Theory Amplitudes*, *JHEP* **06** (2009) 081 [*Erratum ibid.* **11** (2013) 024] [arXiv:0903.1126] [INSPIRE].